Ivanhoe Mines: Platreef Project – Planned Community Centre Site. Farm Turfspruit 241 KR, Mokopane, Limpopo

Ground Penetrating Radar (GPR) Survey for graves

Issue Date:	3 October 2016
Revision No.:	1
Project Number:	TBA

DOCUMENT REFERENCE:

Nienaber, W.C. 2016. Ivanhoe Mines: Platreef Project – Planned Community Centre Site. Farm Turfspruit 241 KR, Mokopane, Limpopo. Ground Penetrating Radar (GPR) Survey for graves. Revision 1. Unpublished report: PGS Heritage.

DECLARATION OF INDEPENDENCE:

The report has been compiled by PGS Heritage, an appointed Heritage Specialist for Ivanhoe Mines. The views stipulated in this report are purely objective and no other interests are displayed during the decision making processes discussed in the Heritage Impact Assessment Process

HERITAGE CONSULTANT: PGS Heritage

CONTACT PERSON: Coen Nienaber

Tel: +27 (0) 12 332 5305

Email: coen@pgsheritage.co.za

SIGNATURE:

DETAILS OF CLIENT

CLIENT: Ivanplats (Pty) Ltd

CONTACT PERSON: Mr Werner Botha

wernerb@ivanplats.com

Report Title	Ivanhoe Mines: Platreef Project – Planned Community Centre Site. Farm Turfspruit 241 KR, Mokopane, Limpopo. Ground Penetrating Radar (GPR) Survey for graves.		
Control	**Name**	**Signature**	**Designation**
Author	Coen Nienaber		Archaeologist
Project Sponsor	Henk Steyn		Managing Director PGS (Pty) Ltd
Reviewed	Mr Werner Botha		Senior Projects Manager, Social & Legal Compliance Ivanplats (Pty) Ltd

EXECUTIVE SUMMARY

Brief

On request from Platreef an assessment of a location at the mine site was conducted by means of Ground Penetrating Radar (GPR) to ascertain whether any graves are present at the indicated area.

Location

The GPR survey area was located inside the Platreef Project fenced area just north west of the main security gate. This area is earmarked for the development of a community centre (Refer map - next page).

Survey methods

A GSSI Utility Scan DF GPR unit was used to conduct the survey. The area was divided into grids and surveyed according to different telemetries and settings.

Findings and recommendations

Anomalies consistent with the presence of possible graves

It is advised that the following localities be <u>ground truthed through archaeological excavation</u> to ascertain whether there are graves present:

1. An anomaly consistent with the possible presence of a grave was observed at Grid10 X6-7Y13,5-15 or grid position X6-8Y93,5-95 taken from point SOP3 as origin and oriented to SOP2(Y) and SOP4(X) (Refer map - next page). It should be considered whether this might be Grave 11A of the graves identified for the Platreef Project.

Localities that might contain human remains

<u>A watching brief at the commencement of construction</u> is advised for the following localities due to the fact that the graves of young children and babies might be present in the house ruins that occur here:

1. Surface indications of previous habitation and subsurface radar anomalies consistent with the presence of building ruins were observed at Grid015 X11,04Y24,03Z0,78 or grid position X31Y1044 from SOP3 (Refer map – next page).
2. And Grid016 X19,09Y13,29Z0,75 or X56Y73 from SOP3 (Refer map – next page).

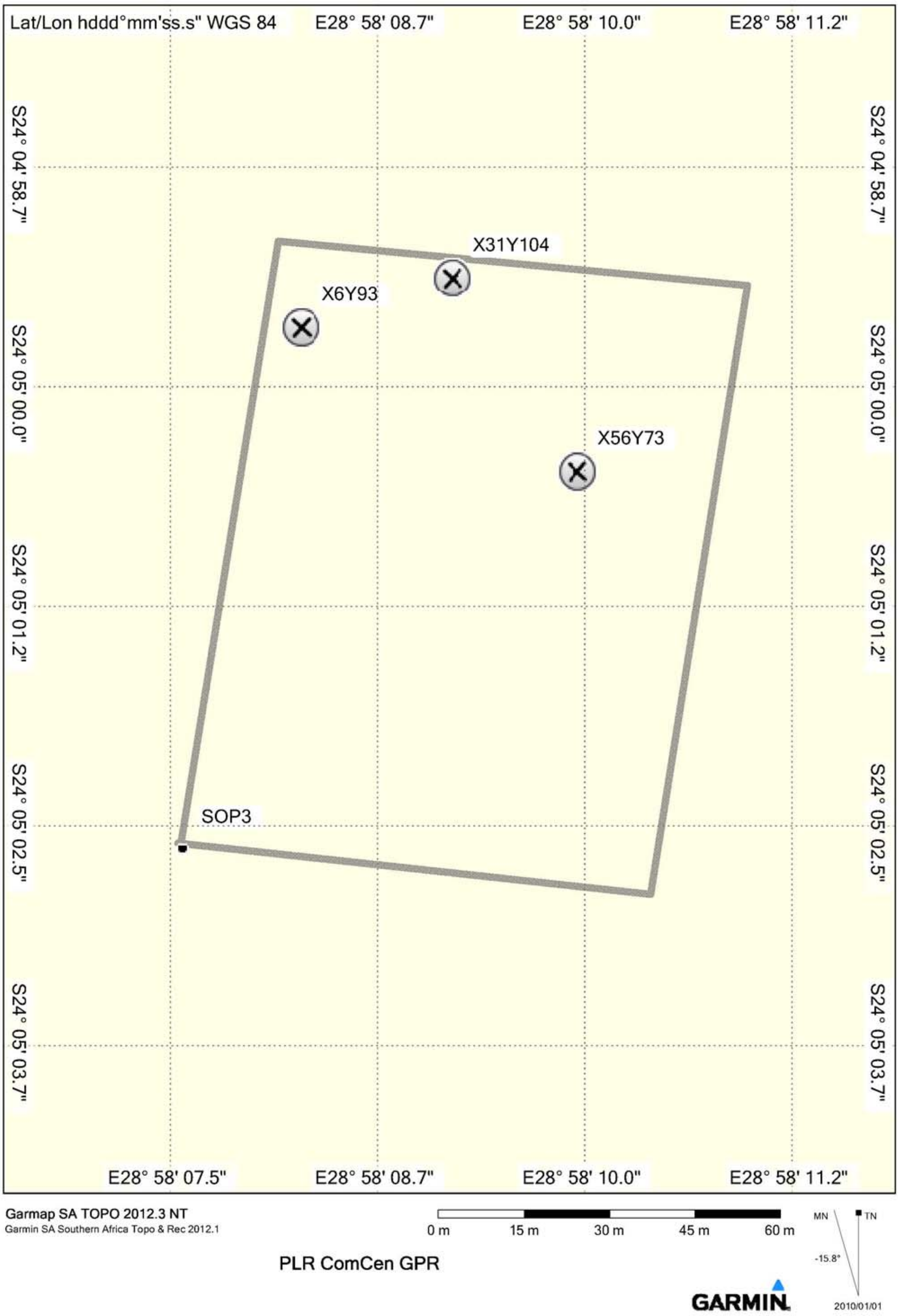
Lat/Lon hddd°mm'ss.s" WGS 84
E28° 58' 08.7"
E28° 58' 10.0"
E28° 58' 11.2"
S24° 04' 58.7"
S24° 05' 00.0"
S24° 05' 01.2"
S24° 05' 02.5"
S24° 05' 03.7"
X31Y104
X6Y93
X56Y73
SOP3
E28° 58' 07.5"
E28° 58' 08.7"
E28° 58' 10.0"
E28° 58' 11.2"
Garmap SA TOPO 2012.3 NT
Garmin SA Southern Africa Topo & Rec 2012.1
0 m
15 m
30 m
45 m
60 m
MN
TN
-15.8°
PLR ComCen GPR
GARMIN
2010/01/01

Table of Contents

1. **BRIEF**

On request from Platreef an assessment of a location at the mine site was conducted by means of Ground Penetrating Radar (GPR) to ascertain whether any graves are present at the indicated area.

2. **INTRODUCTION**

Ground Penetrating Radar (GPR) provides the highest real-time imagery resolution of all land- based geophysical search tools (Schultz, 2012) and has become an established technique in the field of forensic geoscience. In recent years, several studies, focusing on the application of GPR for detecting graves, have emerged; for example Doolittle and Bellantoni (2010), Fiedler et al. (2009), Hansen et al. (2014), Molina et al. (2015), Novo et al. (2011), Pringle et al. (2008), Schultz (2008) and Schultz and Martin (2012). These studies generally fall into one of two categories, those aimed at detecting and/or monitoring unmarked cemetery graves and those aimed at detecting and/or monitoring clandestine graves. GPR is regarded as the best non-intrusive search method for grave detection (Doolittle and Bellantoni, 2010; Schultz and Martin, 2012).

The locality was surveyed and assessed for sub surface radar anomalies that could indicate the possible presence of graves.

3. **LOCATION**

The GPR survey area was located inside the Platreef Project fenced area just north west of the main security gate. This area is earmarked for the development of a community centre.

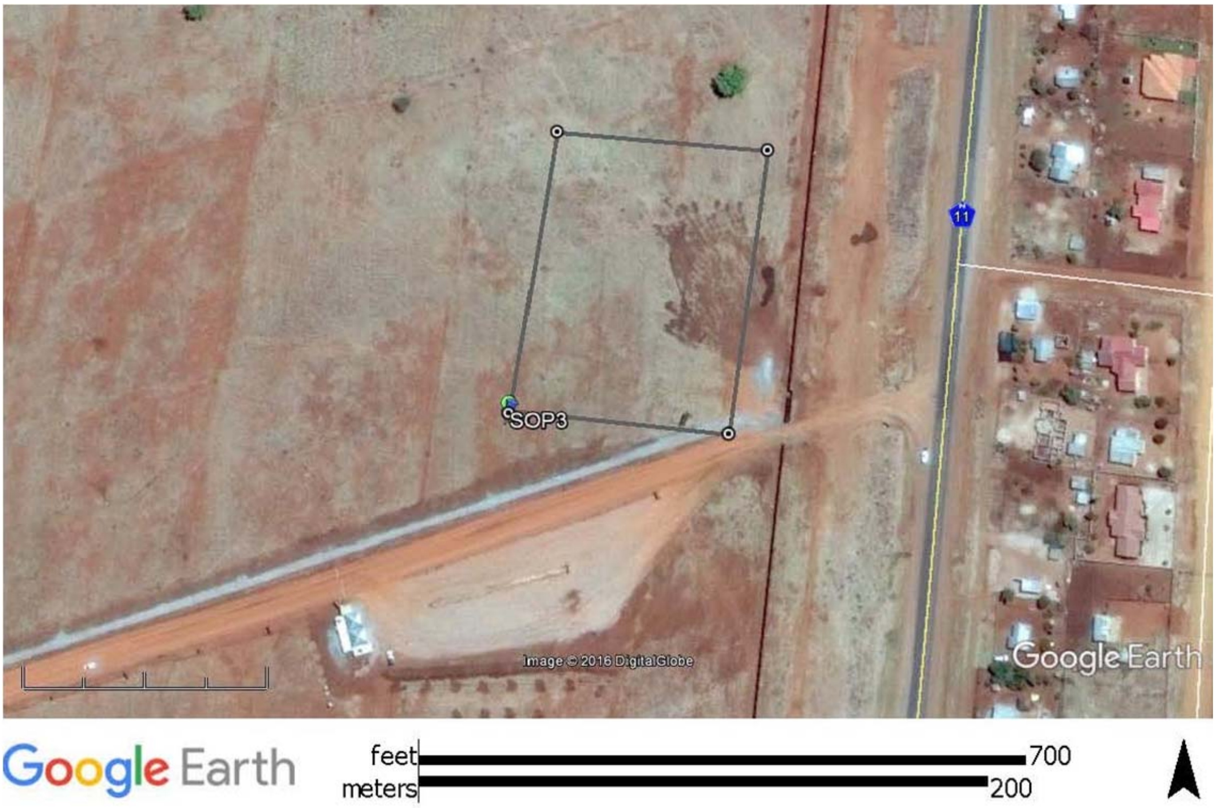

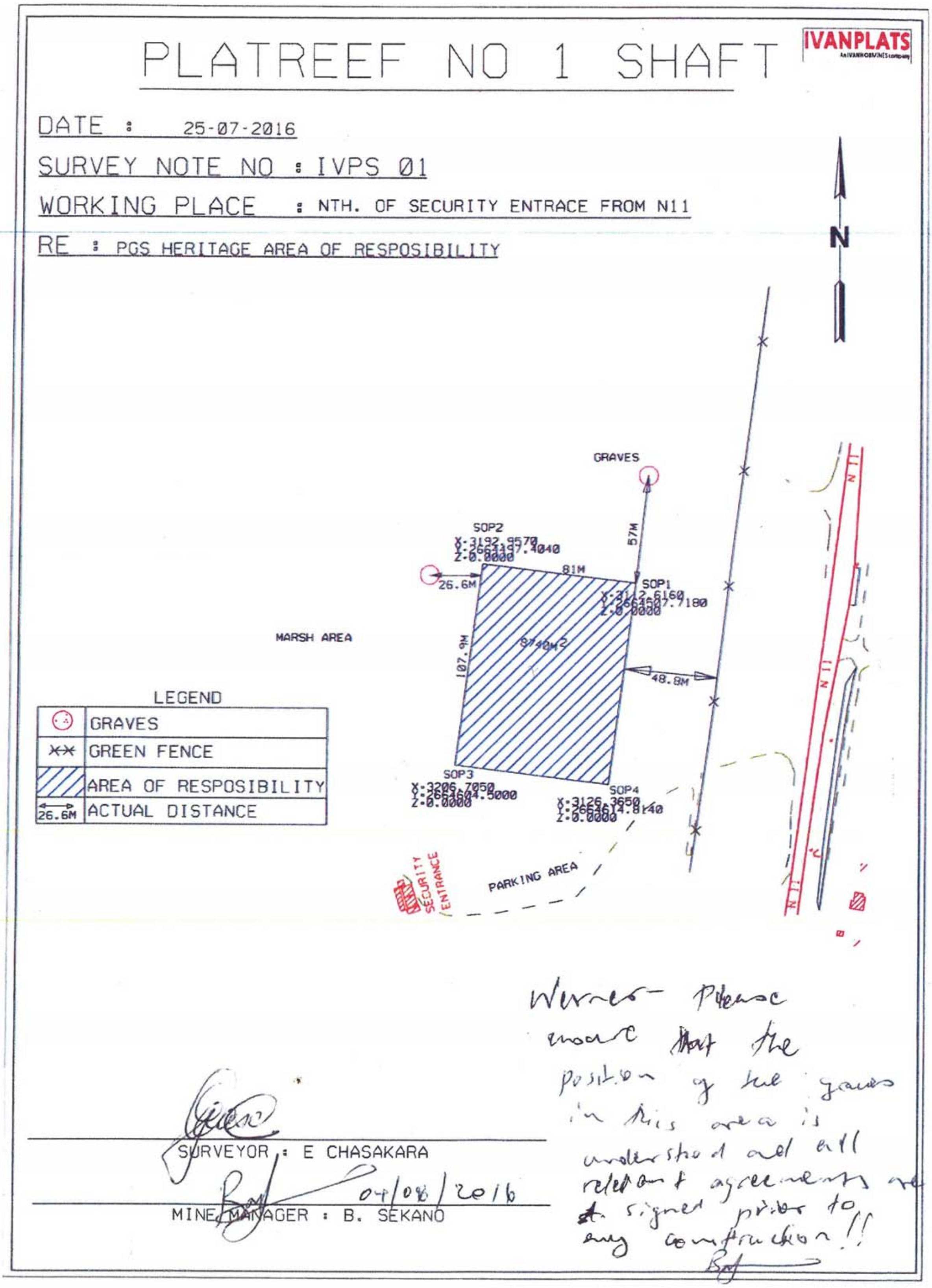

Figure 1. The location of the Platreef community centre area GPR survey.

4. LEGAL COMPLIANCE

Since the survey was not conducted at sites where there were any confirmed heritage resources present a SAHRA permit was not a legal requirement to conduct the investigation. The assessment was designed and conducted to confirm or disprove the possibility that graves might be present in the specific locality. Until such time as the presence of a heritage resource is proven or confirmed; the locality does not comprise a heritage site and is not subject to the requirements of the NHRA (Act 25 of 1999).

5. SURVEY METHODS AND EQUIPMENT

5.1. Using GPR to find and assess graves

For forensic and archaeological geophysical searches all the components of the GPR unit are mounted on a cart. The only interchangeable component is the antenna. The type of antenna that is used is usually dependent on the investigator's preference of vertical resolution over depth of investigation or vice versa and also the soil type. High frequency antennae (800 or 900 MHz) have a reduced depth of investigation but have an increased vertical resolution. This result in an increment in the number of anomalies observed on the reflection profile and makes it difficult to distinguish between a small forensic target and false reflections from roots, trash, stumps, etc. on the reflection profile. The desired target may not be clearly discerned from the clutter produced by these reflection features. Low-frequency antennae (250 MHz) allow for an increased depth of investigation and a reduced vertical resolution and produces less clutter, thus the target will be discerned more easily on the reflection profile. Antennae of 500 or 400 MHz are more popularly used as they are mid-frequency antennae which provide an adequate compromise between vertical resolution and depth of investigation. Antenna choice is also influenced by soil type as the depth of penetration of the electromagnetic (EM) wave is reduced by certain soil types. High percentage clay soils decrease the penetration of radar waves and also dissipate the radar signal (Schultz and Martin, 2012).

The electromagnetic waves that are propagated by the GPR antenna are emitted in a conical pattern and spread out while descending from the antenna into the subsurface matrix being investigated (Schultz, 2012; Dojack, 2012). The subsurface conditions and the frequency of the energy being transmitted into the ground determine the dimensions of the conical pattern. Narrow cones of transmission are produced by high-frequency energy magnitudes, but the energy of the electromagnetic waves is not limited to the centre frequency of the antenna that is being used. GPR dispenses energy in a broad band with a two-octave bandwidth. This basically means that a range of frequencies between one-half and two times the centre frequency will be emitted. These electromagnetic waves display different behaviours such as reflection, diffraction, scattering and focusing, dissipation, dispersion and attenuation as they move through the matrix where they interact with buried materials. The returning (reflected) waves reflect off the boundary of these buried materials and ascend back to the surface where it is detected by the GPR antenna and recorded. Refraction of an electromagnetic wave occurs when it is reflected by subsurface discontinuities and a change in velocity occurs at the interface. This causes a change in direction of the electromagnetic waves through the ground. Generally, the diffraction refers to a spread of waves as they pass through narrow openings. In GPR applications diffraction relates to the phenomenon that produces point source hyperbolas. The hyperbolic image that is produced from a point source is due to the conical pattern of GPR energy which radiates with depth. Scattering of electromagnetic waves is due to the surfaces sloping away from the antenna such as on convex up surfaces, in deep narrow features, and in near vertical features. Conversely, the focusing of electromagnetic waves is when the waves are reflected off surfaces sloping towards the antenna or within shallow wide concave up features. At greater depths, the electromagnetic waves become increasingly dispersed due to the electrical conductivity of subsurface material until such a point that they are fully dissipated, thus there will be no electromagnetic energy that will reflect back to the surface. The rate at which dissipation occurs is relative to the frequency of wave transmission and the properties of the subsurface materials the electromagnetic waves encounter (Dojack, 2012).

GPR allows for real-time imagery to be generated. This makes initial in-field assessments possible (Dupras, et. al., 2012; Schultz, 2012; Doolittle and Bellatoni, 2010). The size, depth and position of the target of interest can be determined. GPR can be used for grave detection under concrete and tarred surfaces and is able to penetrate freshwater, ice comprised of freshwater and snow. The absence of anomalies in an area can exclude areas of non-interest and this will aid in improving the efficiency of search efforts. Such results also provide conclusive findings when verifying the existence of graves reported at a locality. Three-dimensional GPR data reconstructions or models can be used to determine the context, spatial arrangement of the object and also stratigraphy of an area interest (Schultz, 2012; Hansen, et. al., 2014). However, the GPR equipment require level terrain to operate on (Dupras, et. al., 2012; Schultz, 2012; Doolittle and Bellatoni, 2010; Shultz and Martin, 2012; Dojack, 2012). There must also be sufficient contrast between the grave and soil in order for successful grave detection to occur (Dupras, 2012) and the visibility of targets can be inhibited due to clutter that is caused by buried debris, rocks and roots (Schultz, 2012). This will result is an increased amount of noise being observed on the GPR profile and can lead to misinterpretation of anomalies (Schutz and Martin, 2012). The radar waves of GPR become very rapidly attenuated in soil types that are clay–rich and saline (Dojack, 2012).

The GPR unit is operated by the investigator while walking at a slow pace. The antenna's receiving unit gathers the reflected data as a series of discrete waves that are produced by the radar transmission process. The GPR results or observations comprises of the reflected electromagnetic wave traces that are generated along the transect or gridline. A GPR profile is a two-dimensional or cross-section image of the subsurface area that displays time or depth along the vertical axis and length of the transect along the horizontal axis. The determination of depth of a subsurface object is obtained by using two methods namely, relative dielectric permittivity value of the soil being surveyed and also through the use of a reflected-wave method. The relative dielectric value of a material is deduced by how much radar energy will be transmitted at a particular depth through that material. The limitation of this method is that soil properties may not be homogenous across a survey. This will result in obtaining only an estimate depth value across the site. The reflected-wave is regarded as the as the most accurate method to determine depth. This method involves the analyses of reflections at known depths on the GPR profile that allow for the calculation of average–velocity waves. The GPR profile does not display an actual image of a buried body or skeleton when a grave has been detected. A reflection, which appears as a series of hyperbolic curves, that is the result of a buried feature are observed instead and this is commonly known as an anomaly. The buried feature is situated at the apex of the anomaly and the series of the hyperbolae can extend deeper than the detected buried feature. It is an essential skill that an operator recognizes an anomaly or the series of hyperbolae curves when conducting in-field assessments (Schultz, 2012). The information that is obtained from a GPR survey can further be processed by means of various processing software that filter out unprocessed profiles termed noise or multiples (Schultz, 2012; Conyers, 2006). This will increase the resolution of the GPR profile and the chances of observing buried subsurface materials that were obscured by the noise (Schultz, 2012).

5.2. Equipment specification

A GSSI Utility Scan DF GPR unit with the following specifications was used:

Controller			
System	Panasonic Toughpad ® FZ-G1		
Data Storage Internal Memory	128 GB SSD		
Display	Enhanced 10.1" WUXGA 1920x1200 with LED backlighting		
Processor	Intel® Core i5-2557M vPro		
Ports	USB 3.0, Ethernet and Serial		
Batteries	Li-Ion battery pack (10.8 V typical 9300 mAh)		
Operating Temperature	-28°C to 60°C (-20°F to 140°F)		
Weight	2.7 kg (6 lbs)		
Environmental	IP65		
Drop Spec	MIL-STD-810G		
GSSI System Software			
Scan Rate	150 scans/sec at 512 samples/scan		
Scan Intervals	50 or 100 scans/meter (15 or 30 scans/foot)		
Output Data Resolution	32-bit		
Operating Mode	Survey Wheel		
Depth Ranges	Metric		
	High Frequency	Low Frequency	
	0.50 m	1 m	
	0.75 m	2 m	
	1 m	3 m	
	2 m	4 m	
	3 m	5 m	
	English		
	High Frequency	Low Frequency	
	12 in	3 ft	
	18 in	6 ft	
	3 ft	9 ft	
	6 ft	12 ft	
	9 ft	15 ft	
System Speed	up to 600 kHz, 200 kHz in North America		
Data Collection Speed	up to 10 km/h (6.25 mph)		
Gain	Manual or automatic, 1-8 gain points (-42 to + 126 dB)		
Real-time Filters	Stacking, Background Removal		
Advanced Real-time Filter	Signal floor tracking		
Display Mode	**Linescan Mode:** high frequency data only or low frequency data only displayed		

	Dual Mode: high and low frequency data displayed in split screen view **Blend Mode:** high and low frequency data combined in single view
Data Format	RADAN® (.dzt)
Diagnostic	GPS status and battery
Digital Dual Frequency Smart Antenna	
Number of Hardware Channels	2 (two)
Frequencies	300 and 800 MHz
Typical Range	4 m / 12 ft
Maximum Range	7 m / 21 ft
Connectors	Digital control, power, survey wheel, marker, serial RS232, accessory connector
GPS	Data stored internally
Operating Temperature	-10°C to 50°C (14°F to 122°F)
Weight	5 kg (12 lbs)
Dimensions	33.5 x 31 x 15 cm (13.2 x 12.2 x 5.9 in)
Environmental	IP65
Cart	
Model 655	4-wheel, compact survey cart Internal, integrated survey wheel encoder Removable, 12-inch wheels Compact, weather resistant design Antenna centerline to front of cart: 38.2 cm (15 in) Dimensions: 61.7 x 100 x 102.4 cm (24.3 x 39.4 x 40.3 inches) **Total System Weight:** 29 kg (66 lbs)

http://www.geophysical.com/utilityscandf.htm (Accessed 2015/11/02)

5.3. Grid

Figure 2. The Platreef Community Centre GPR survey area.

The area included in the survey was an old agricultural field with some cultural features, such as habitation remains, visible on the surface (Refer Figure 2). A large part of the surface of the area was previously graded after it was no longer in use as an agricultural field (Refer Figure 1).

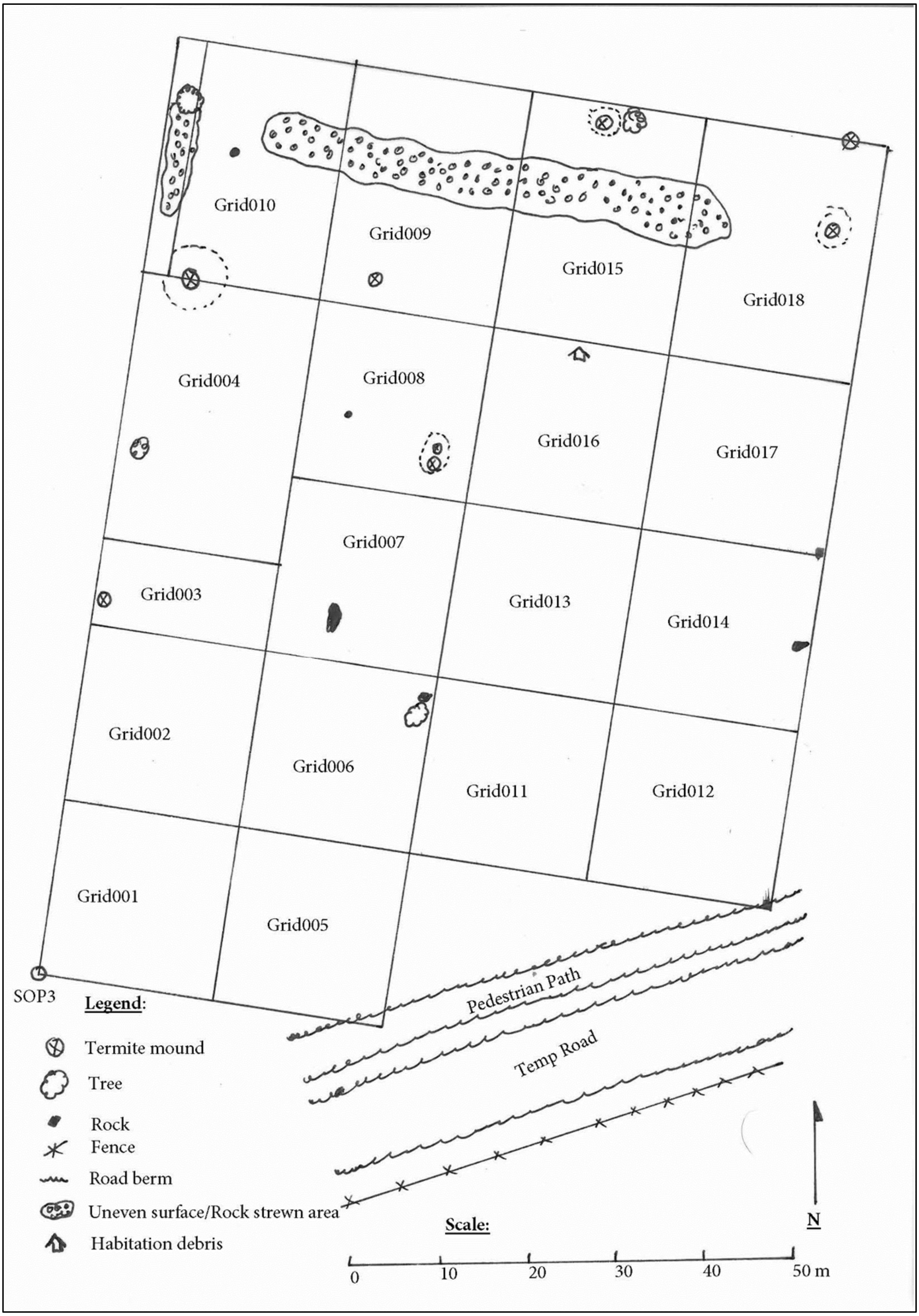

Figure 3. Schematic of the Platreef Community Centre GPR survey grid layout.

The indicated survey area was divided into grids as follows (Refer Figure 3):

Grid datum: S24° 05' 02.6" E28° 58' 07.6" (GPS).

- Grid001 - 20 m by 20 m NNE of SOP3 at 0.5 m intersects, zigzag in both X and Y directions.
- Grid002 - 20 m by 20 m NNE of Grid 001 at 0.5 m intersects, zigzag in both X and Y directions.
- Grid003 - 10 m by 20 m NNE of Grid 002 at 0.5 m intersects, zigzag in both X and Y directions.
- Grid004 - 30 m by 20 m NNE of Grid 003 at 0.5 m intersects, zigzag in both X and Y directions.
- Grid005 - 20 m by 20 m ESE of Grid 001 at 0.5 m intersects, zigzag in both X and Y directions.
- Grid006 - 20 m by 20 m NNE of Grid 005 at 0.5 m intersects, zigzag in both X and Y directions.
- Grid007 - 20 m by 20 m NNE of Grid 006 at 0.5 m intersects, zigzag in both X and Y directions.
- Grid008 - 20 m by 20 m NNE of Grid 007 at 0.5 m intersects, zigzag in both X and Y directions.
- Grid009 - 27 m by 20 m NNE of Grid 008 at 0.5 m intersects, zigzag in both X and Y directions.
- Grid010 - 27 m by 17 m NNE of Grid 004 at 0.5 m intersects, zigzag only in X direction.
- Grid011 - 20 m by 20 m ESE of Grid006 in 1m transects, zigzag in both X and Y directions.
- Grid012 - 20 m by 20 m ESE of Grid011 in 1m transects, zigzag in both X and Y directions.
- Grid013 - 20 m by 20 m NNE of Grid011 in 1m transects, zigzag in both X and Y directions.
- Grid014 - 20 m by 21 m ESE of Grid013 in 1m transects, zigzag in both X and Y directions.
- Grid015 - 27 m by 20 m ESE of Grid009 in 1m transects, zigzag in both X and Y directions.
- Grid016 - 20 m by 20 m NNE of Grid013 in 1m transects, zigzag in both X and Y directions.
- Grid017 - 20 m by 21 m ESE of Grid016 in 1m transects, zigzag in both X and Y directions.
- Grid018 - 27 m by 21 m ESE of Grid015 in 1m transects, zigzag in both X and Y directions.
- Line 001-022 - Parallel to the road berms in the SE part of the survey area at 0.5 m intervals as far as this was allowed by the infrastructure, zigzag starting just SE of the pedestrian road berm.
- Line023 - Not used – no data recorded.
- Line024-043 - Starting just NNE of the pedestrian road berm and proceeding N at 0.5 m intervals in zigzag manner to cover the remaining area.

5.4. Survey parameters

In order to obtain the best possible results the following parameters were applied in different grids:

- Grid001

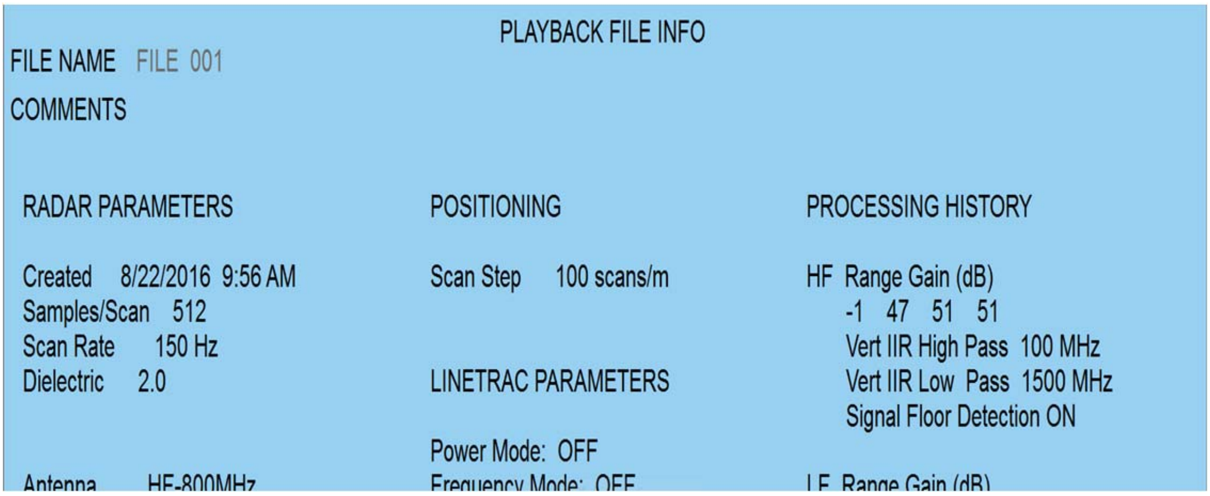

- Grid002 and 003

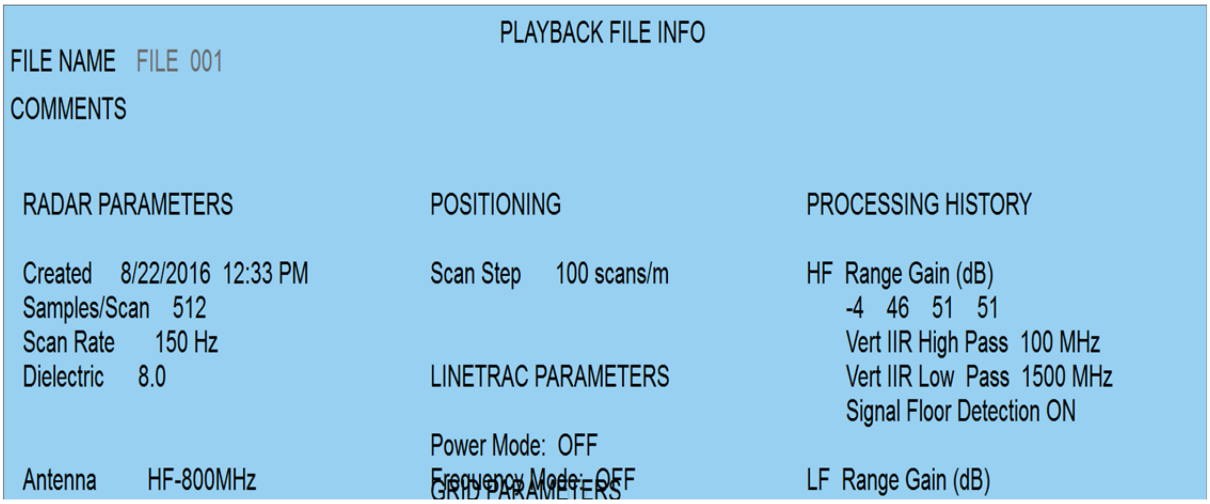

- Grid004 and 005

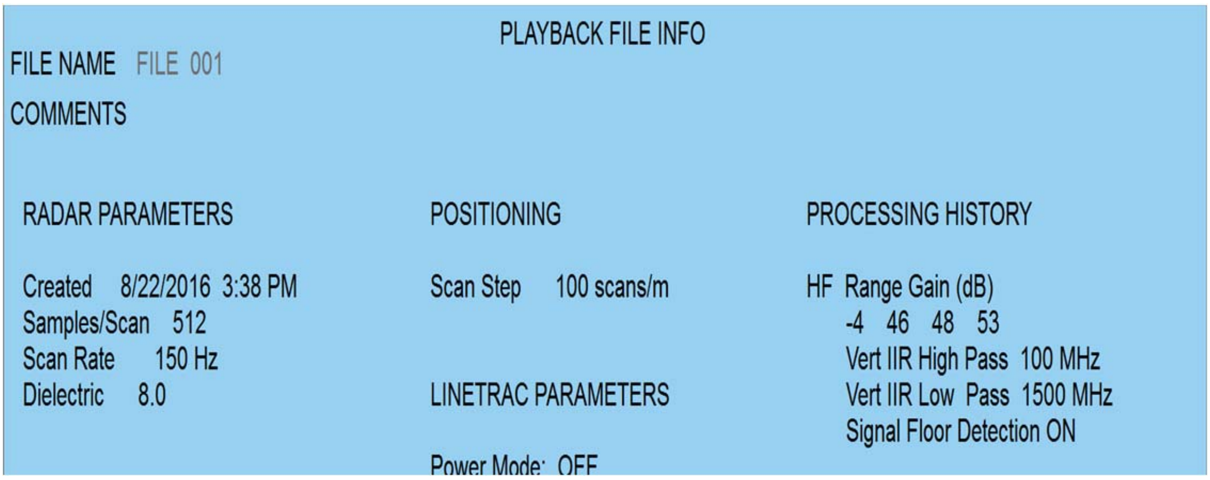

- Grid006

PLAYBACK FILE INFO

FILE NAME FILE 001

COMMENTS

RADAR PARAMETERS	POSITIONING	PROCESSING HISTORY
Created 8/23/2016 10:39 AM	Scan Step 100 scans/m	HF Range Gain (dB)
Samples/Scan 512		-1 56 58 58
Scan Rate 150 Hz		Vert IIR High Pass 100 MHz
Dielectric 14.0	LINETRAC PARAMETERS	Vert IIR Low Pass 1500 MHz
		Signal Floor Detection ON
	Power Mode: OFF	

- Grid007

PLAYBACK FILE INFO

FILE NAME FILE 001

COMMENTS

RADAR PARAMETERS	POSITIONING	PROCESSING HISTORY
Created 8/23/2016 12:22 PM	Scan Step 100 scans/m	HF Range Gain (dB)
Samples/Scan 512		-2 53 58 58
Scan Rate 150 Hz		Vert IIR High Pass 100 MHz
Dielectric 14.0	LINETRAC PARAMETERS	Vert IIR Low Pass 1500 MHz
		Signal Floor Detection ON
	Power Mode: OFF	

- Grid008

PLAYBACK FILE INFO

FILE NAME FILE 001

COMMENTS

RADAR PARAMETERS	POSITIONING	PROCESSING HISTORY
Created 8/23/2016 1:31 PM	Scan Step 100 scans/m	HF Range Gain (dB)
Samples/Scan 512		-2 52 55 55
Scan Rate 150 Hz		Vert IIR High Pass 100 MHz
Dielectric 14.0	LINETRAC PARAMETERS	Vert IIR Low Pass 1500 MHz
		Signal Floor Detection ON
	Power Mode: OFF	
Antenna HF-800MHz	Frequency Mode: OFF	LF Range Gain (dB)

- Grid009 and 010

PLAYBACK FILE INFO

FILE NAME FILE 001

COMMENTS

RADAR PARAMETERS

Created 8/23/2016 3:25 PM
Samples/Scan 512
Scan Rate 150 Hz
Dielectric 14.0

Antenna HF-800MHz

POSITIONING

Scan Step 100 scans/m

LINETRAC PARAMETERS

Power Mode: OFF
Frequency Mode: OFF

PROCESSING HISTORY

HF Range Gain (dB)
-3 53 55 55
Vert IIR High Pass 100 MHz
Vert IIR Low Pass 1500 MHz
Signal Floor Detection ON

LF Range Gain (dB)

- Grid011 and 012

PLAYBACK FILE INFO

FILE NAME FILE 001

COMMENTS

RADAR PARAMETERS

Created 8/24/2016 9:55 AM
Samples/Scan 512
Scan Rate 150 Hz
Dielectric 14.0

Antenna HF-800MHz

POSITIONING

Scan Step 100 scans/m

LINETRAC PARAMETERS

Power Mode: OFF
Frequency Mode: OFF

PROCESSING HISTORY

HF Range Gain (dB)
1 54 61 61
Vert IIR High Pass 100 MHz
Vert IIR Low Pass 1500 MHz
Signal Floor Detection ON

LF Range Gain (dB)

- Grid013 and 014

PLAYBACK FILE INFO

FILE NAME FILE 001

COMMENTS

RADAR PARAMETERS

Created 8/24/2016 11:33 AM
Samples/Scan 512
Scan Rate 150 Hz
Dielectric 14.0

Antenna HF-800MHz

POSITIONING

Scan Step 100 scans/m

LINETRAC PARAMETERS

Power Mode: OFF
Frequency Mode: OFF

PROCESSING HISTORY

HF Range Gain (dB)
0 51 58 58
Vert IIR High Pass 100 MHz
Vert IIR Low Pass 1500 MHz
Signal Floor Detection ON

LF Range Gain (dB)

- Grid015

PLAYBACK FILE INFO

FILE NAME FILE 001

COMMENTS

RADAR PARAMETERS

Created 8/25/2016 8:45 AM
Samples/Scan 512
Scan Rate 150 Hz
Dielectric 14.0

POSITIONING

Scan Step 100 scans/m

LINETRAC PARAMETERS

Power Mode: OFF

PROCESSING HISTORY

HF Range Gain (dB)
1 55 62 62
Vert IIR High Pass 100 MHz
Vert IIR Low Pass 1500 MHz
Signal Floor Detection ON

- Grid016

PLAYBACK FILE INFO

FILE NAME FILE 001

COMMENTS

RADAR PARAMETERS

Created 8/25/2016 9:25 AM
Samples/Scan 512
Scan Rate 150 Hz
Dielectric 14.0

POSITIONING

Scan Step 100 scans/m

LINETRAC PARAMETERS

Power Mode: OFF

PROCESSING HISTORY

HF Range Gain (dB)
2 51 60 60
Vert IIR High Pass 100 MHz
Vert IIR Low Pass 1500 MHz
Signal Floor Detection ON

- Grid017

PLAYBACK FILE INFO

FILE NAME FILE 001

COMMENTS

RADAR PARAMETERS

Created 8/25/2016 10:35 AM
Samples/Scan 512
Scan Rate 150 Hz
Dielectric 14.0

POSITIONING

Scan Step 100 scans/m

LINETRAC PARAMETERS

Power Mode: OFF

PROCESSING HISTORY

HF Range Gain (dB)
0 52 58 58
Vert IIR High Pass 100 MHz
Vert IIR Low Pass 1500 MHz
Signal Floor Detection ON

- Grid018

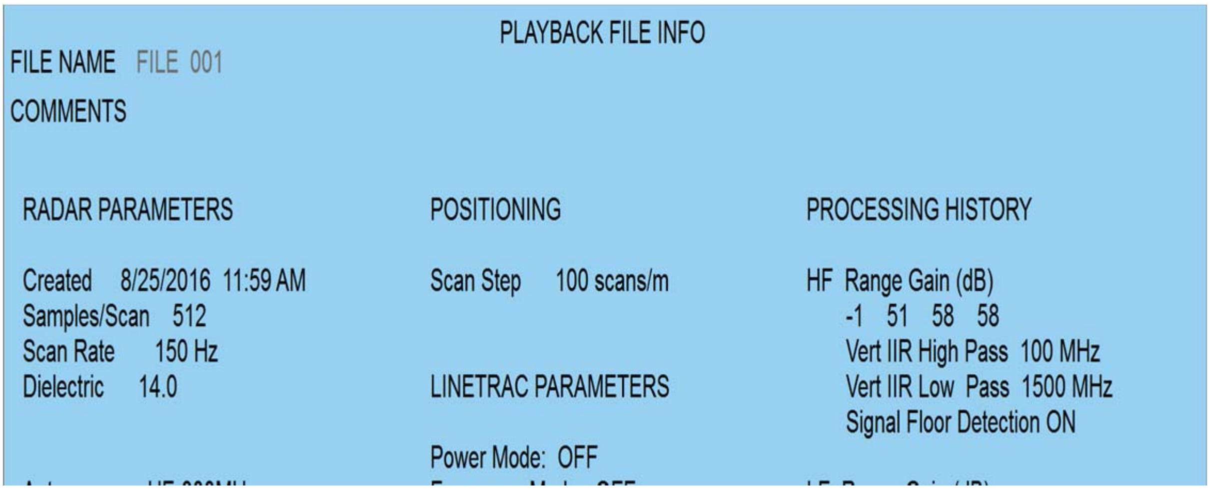

5.5. Data processing and visualization

2D and 3D analyses were performed on the various GPR data sets. For the initial 2D analyses the REFLEXW software (by Sandmeier Scientific Software) was used for some datasets. Time-zero corrections were applied to the data, followed by additional standard processing steps, including dewow filtering and automatic gain control (AGC). Where data was processed in real time the steps are included with the visualizations presented in this report (See PROCESSING HISTORY in table on page 9 and onwards).

Some profiles were also imported into Sensors & Software's GFP_Edit software where the geometry of the 3D grid surveys were edited and the input files for the depth slice module Ekko_Mapper was generated where this was necessary to enhance the results. Additional processing steps applied during depth slice generation included amplitude equalisation gain, velocity-based migration, envelope filtering and background subtraction where applicable. In most cases the on-board real time processing was deemed sufficient and is included in this report as such.

The visualizations presented in this report are with the equipment firmware, by means of screen capture, unless indicated differently.

6. RESULTS

6.1. General Radar sub surface profile of the area

The general radar characteristics of the areas show a plough zone to an average depth of about 50 cm below surface overlaying a silt layer. The sub surface soil geology of the area presents as homogeneous in terms of ground penetrating radar properties.

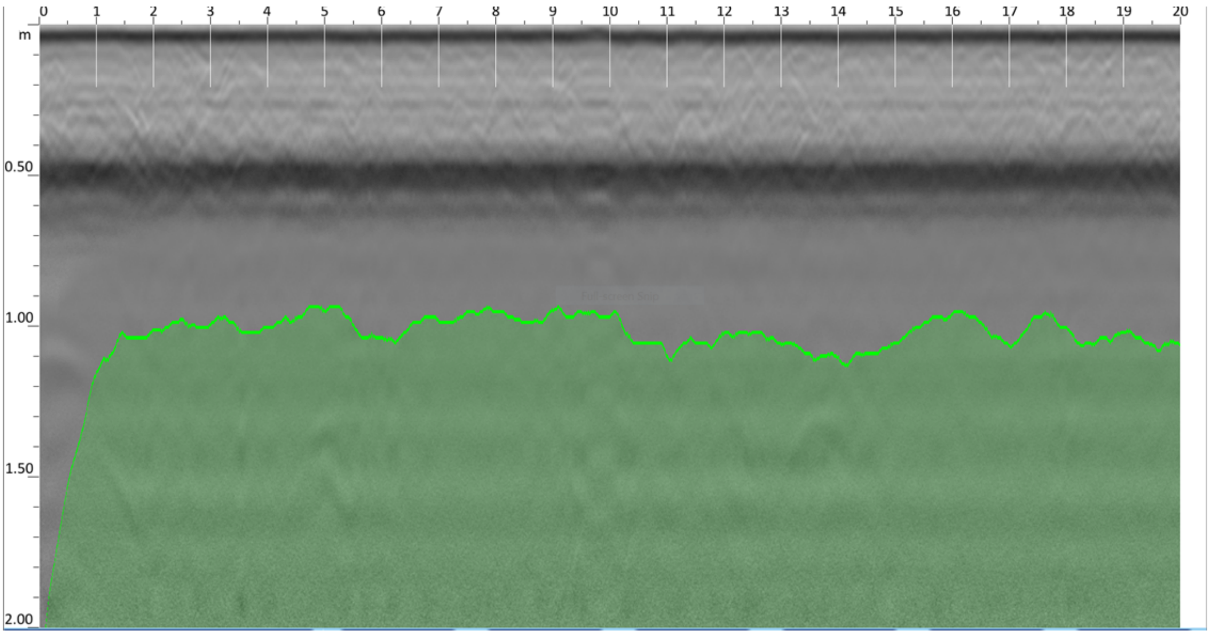

Figure 4. General radar properties of the survey area.

6.2. Grid001

No radar anomalies consistent with the presence of graves were observed in the 3D reconstruction for this grid.

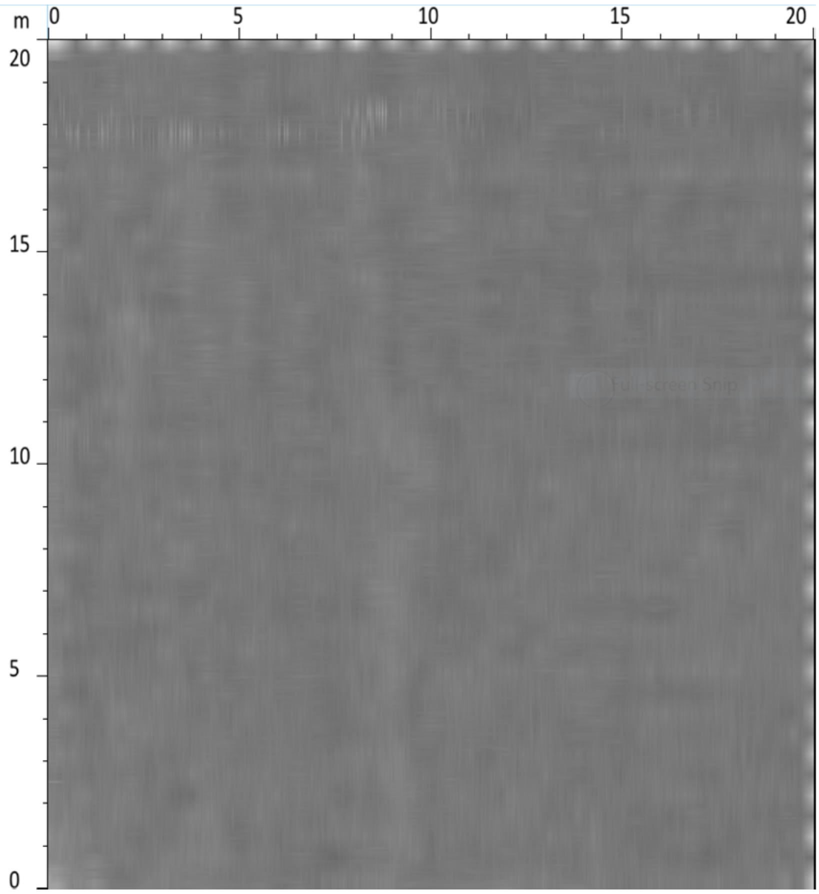

Figure 5. 3D visualization for Grid001.

6.3. Grid002

Possible anomalies were visible at a depth of approximately 0.75 m in the Z aspect of the 3D reconstruction of data for this grid:

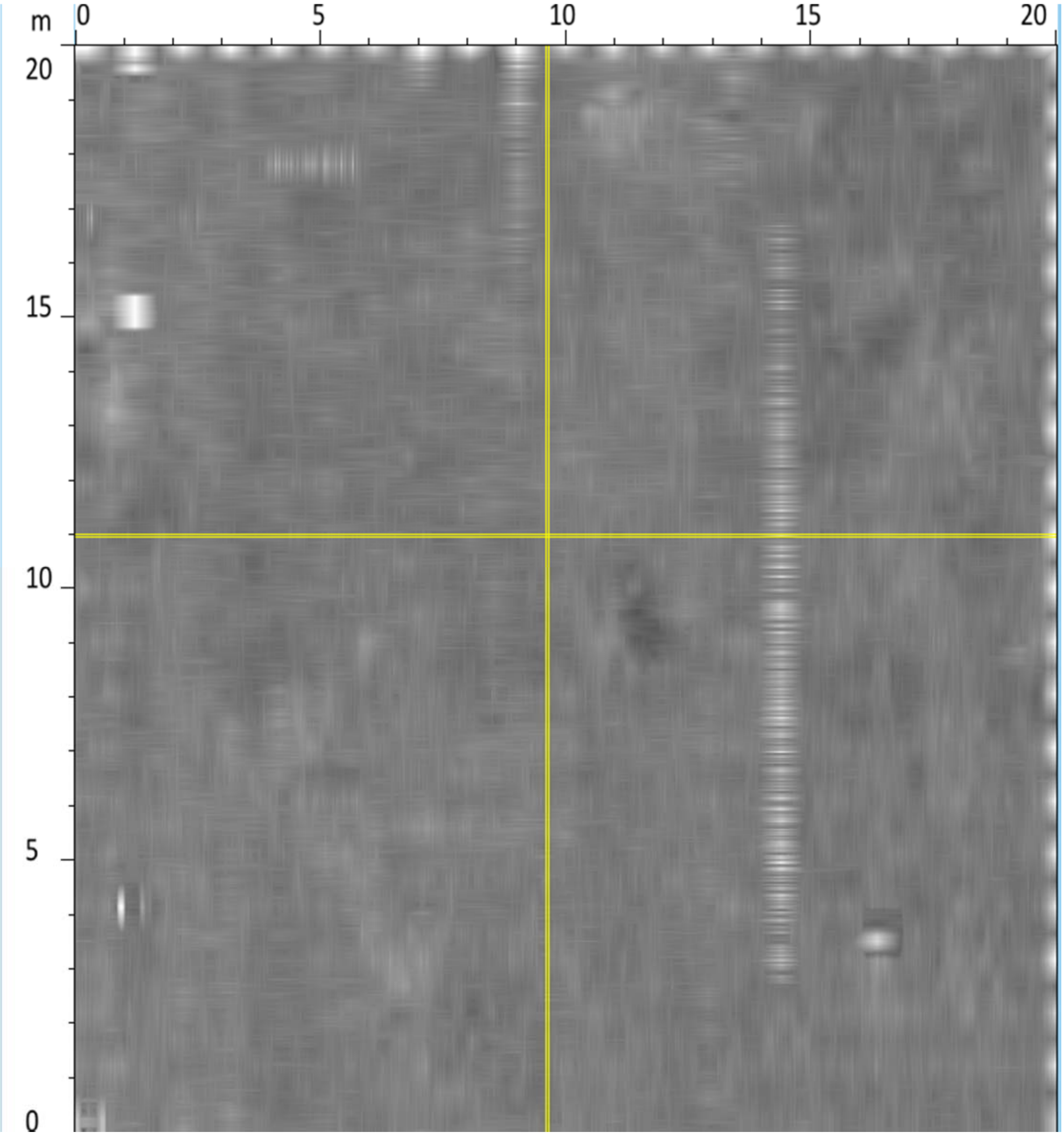

Figure 6. Grid002 3D visualization of data.

- At X16,52Y16,26 m but no corresponding anomaly is visible in the X aspect.

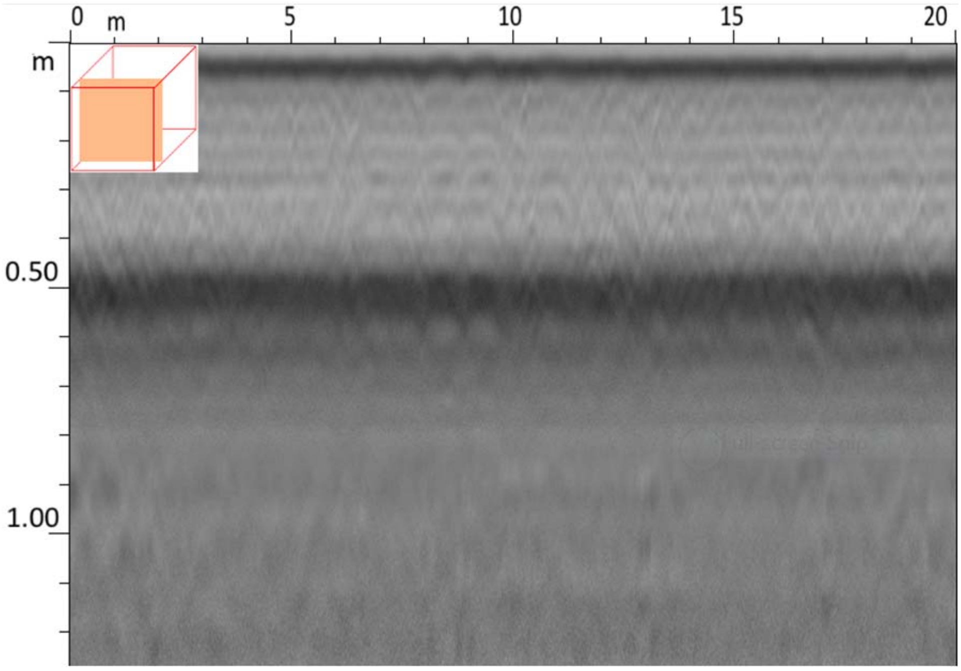

Figure 7. Grid002 anomaly 1 X profile view.

- At X1,29Y4,61 m but with no corresponding anomaly visible in the Y aspect.

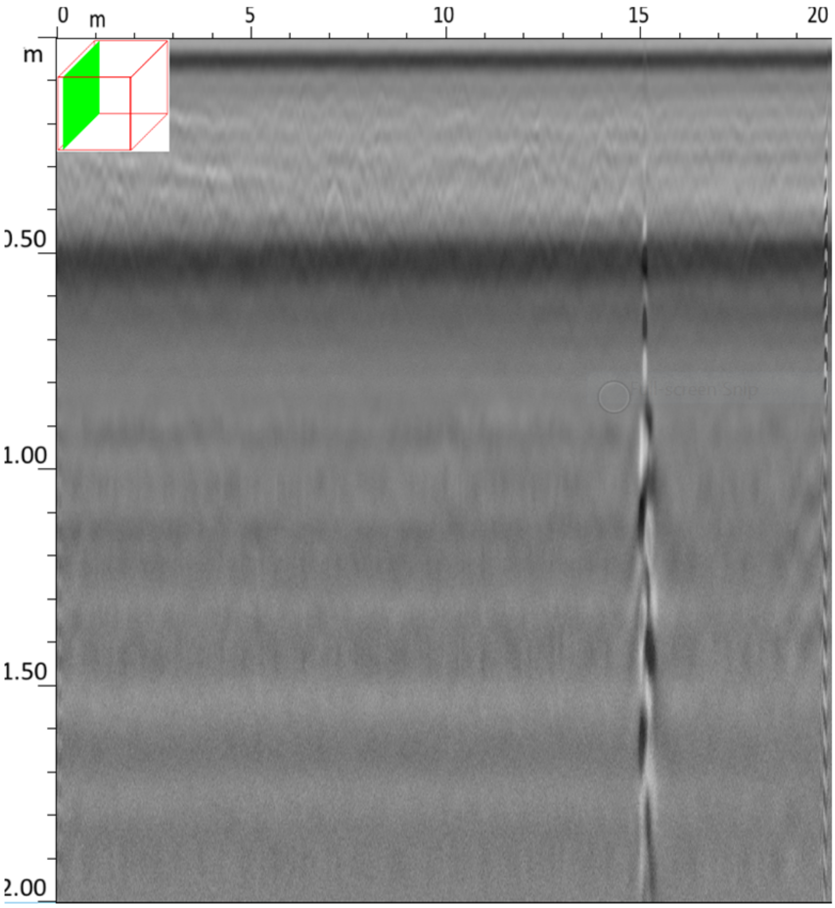

Figure 8. Grid002 anomaly 2 Y profile view.

- At X1,12Y15.80 m and showing a narrow deep anomaly visible in the Y aspect but which is not consistent with a possible grave.

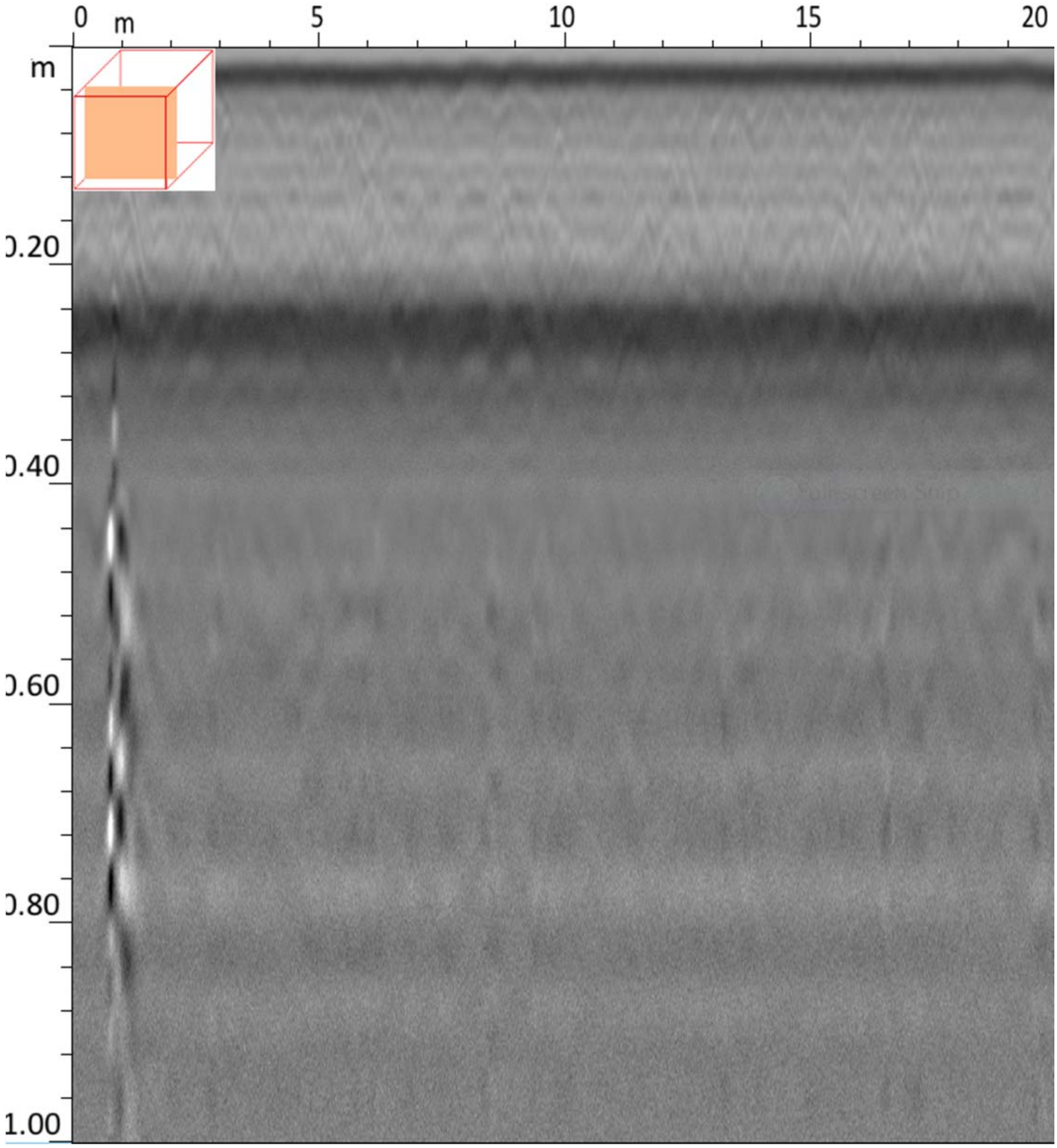

Figure 9. Grid002 anomaly 3 X profile view.

6.4. Grid003

No radar anomalies were visible in the 2D profile data for this grid.

6.5. Grid004

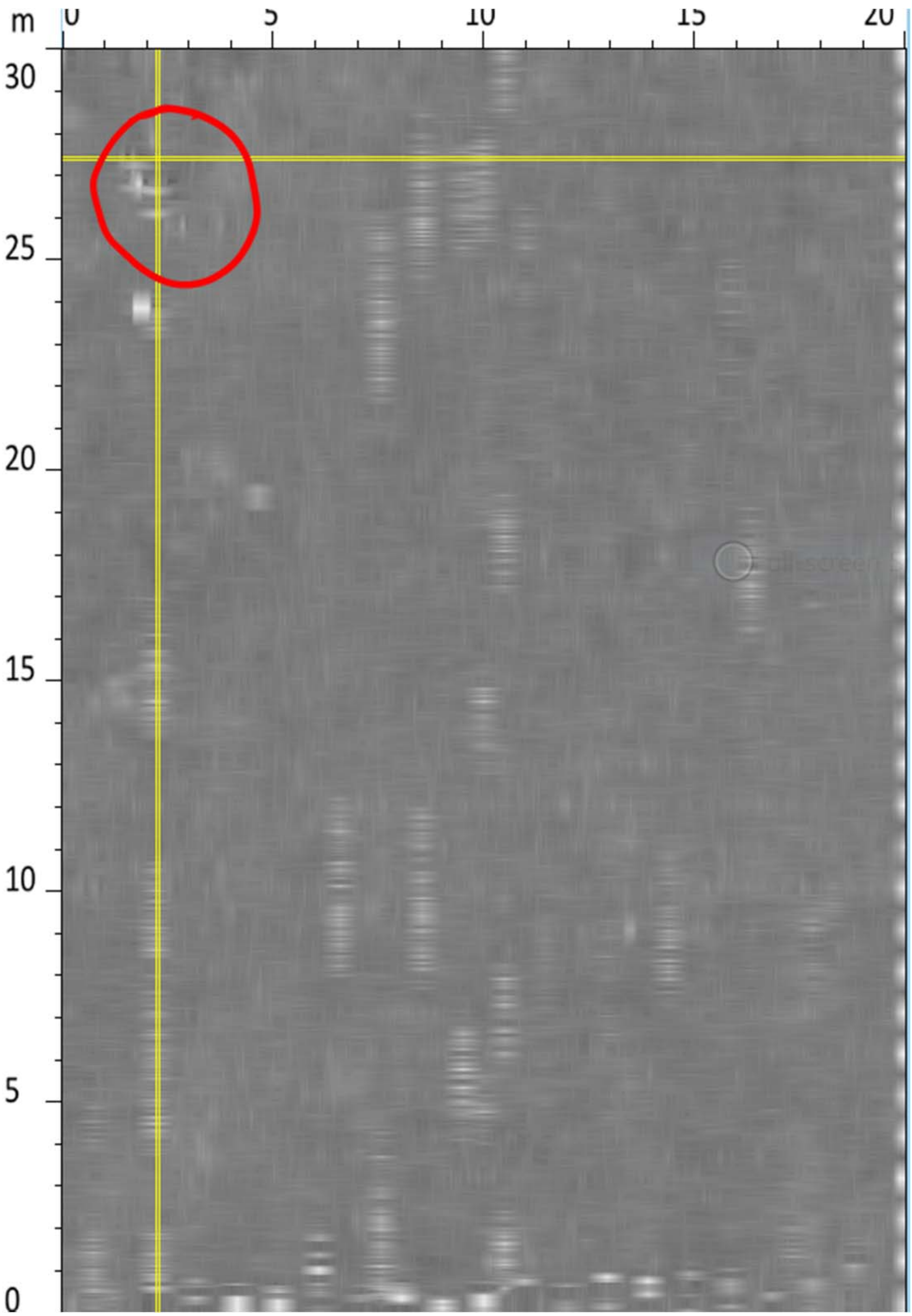

Figure 10. 3D visualization of data for Grid004.

Anomalies were observed in the 3D reconstruction of data for this grid:

- X2,28Y2,61m – the X and Y profile aspects for this anomaly is not consistent with the possible presence of a grave and also corresponds with a termite nest visible on the surface.

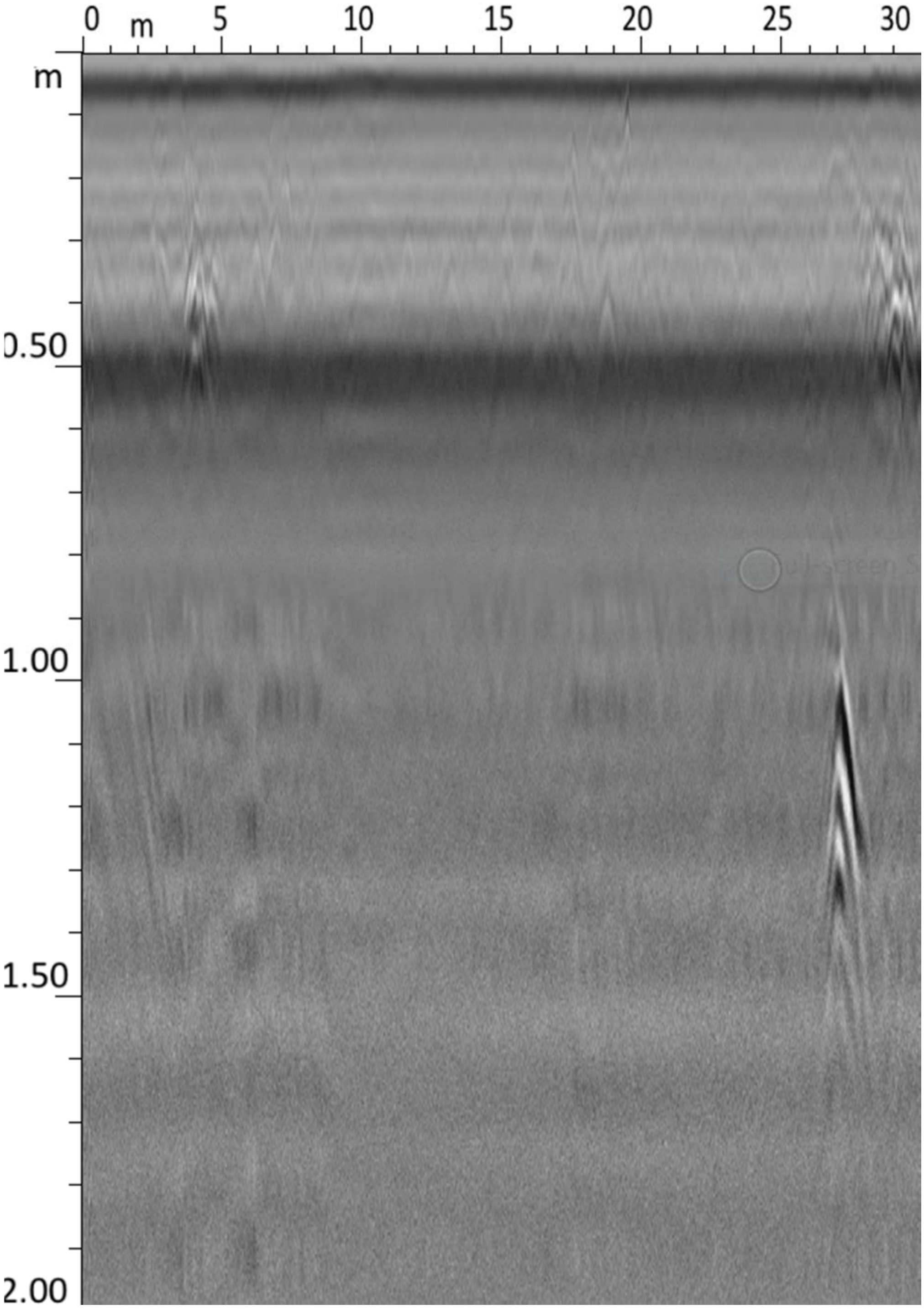

Figure 11. Grid004 anomaly in X profile view.

6.6. Grid005

No anomalies were observed in the 2D profiles from this grid.

6.7. Grid006

No radar anomalies consistent with the presence of graves were observed in the 3D reconstruction for this grid.

6.8. Grid007

Anomalies were observed in the 3D reconstruction of data for this grid:

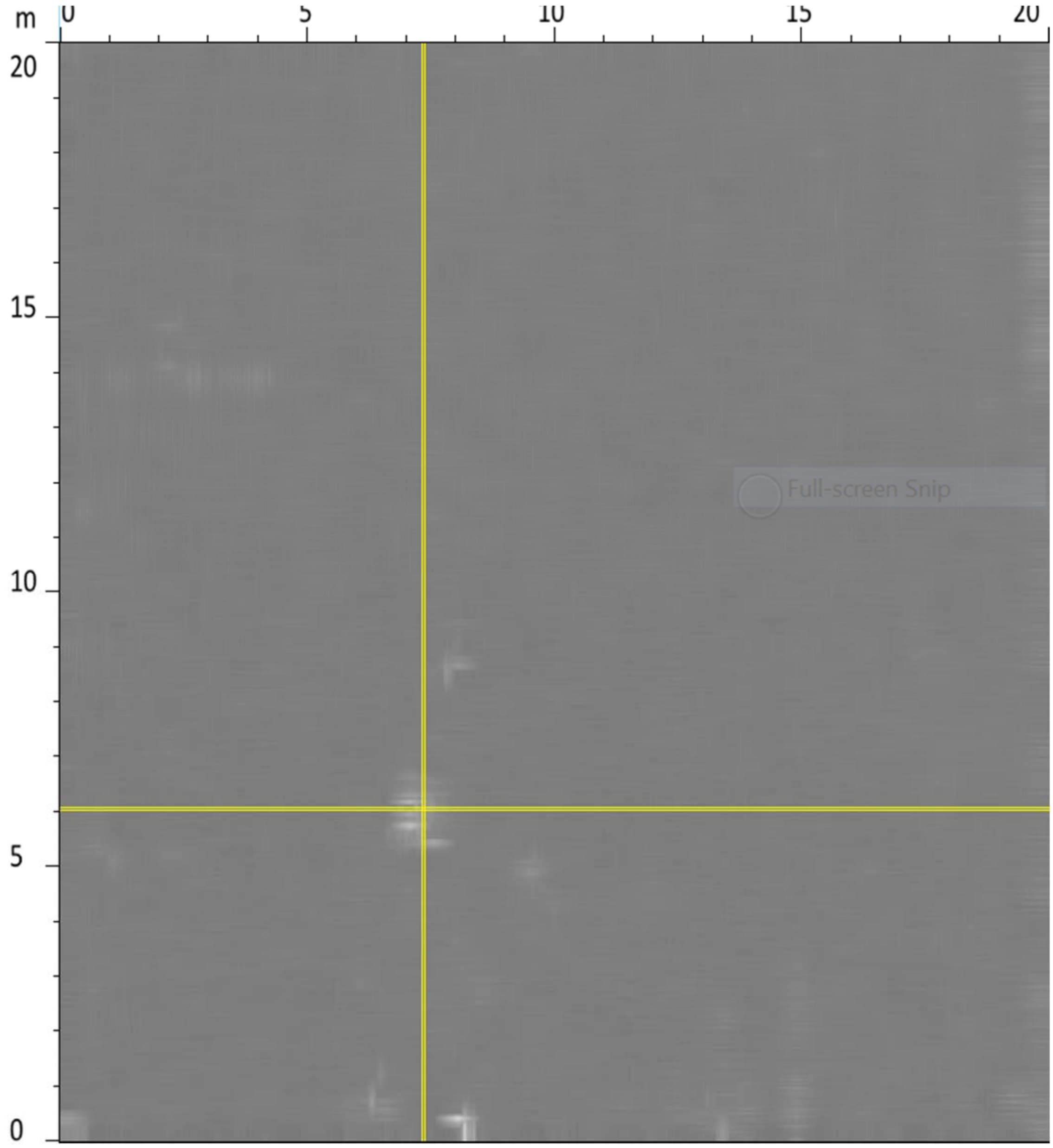

Figure 12. Grid007 3D visualization of data.

- X7,36Y7,36 - this corresponds with a rock visible on the surface (Figure 3) and also in the Y aspect profile radargraph.

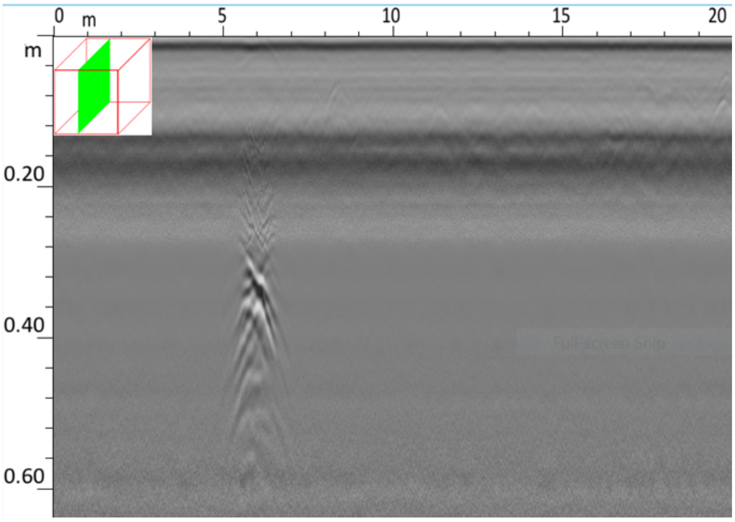

Figure 13. Grid007 anomaly Y aspect profile view.

6.9. Grid008

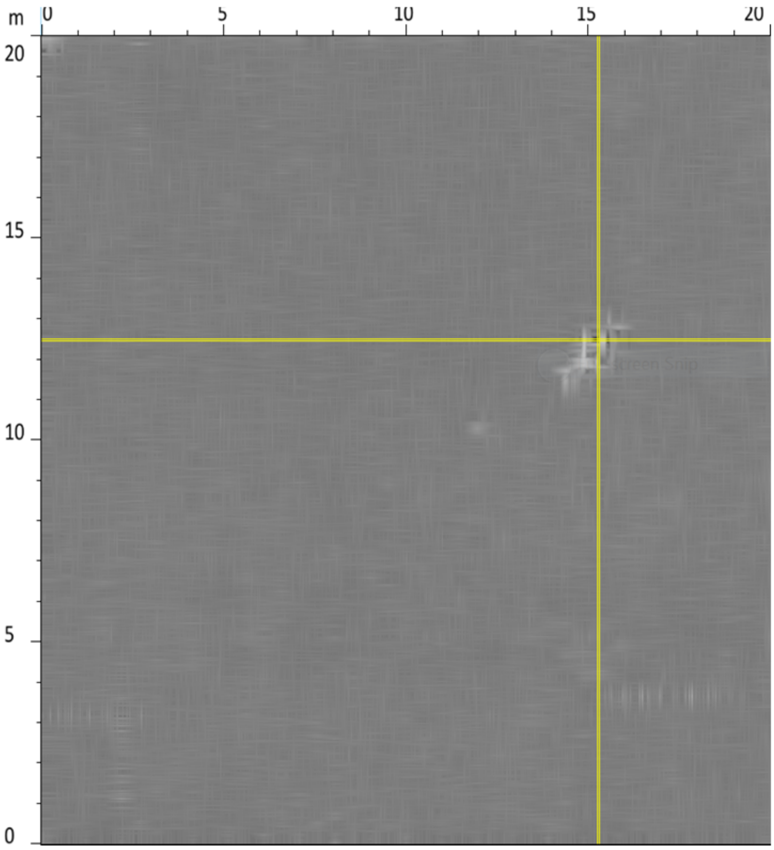

Figure 14. 3D visualization of data for Grid008.

Anomalies were visible in the 3D reconstruction of data from this grid.

X15.29Y7.54 – The y aspect profile shows a shallow anomaly open to the surface, most probably a termite nest.

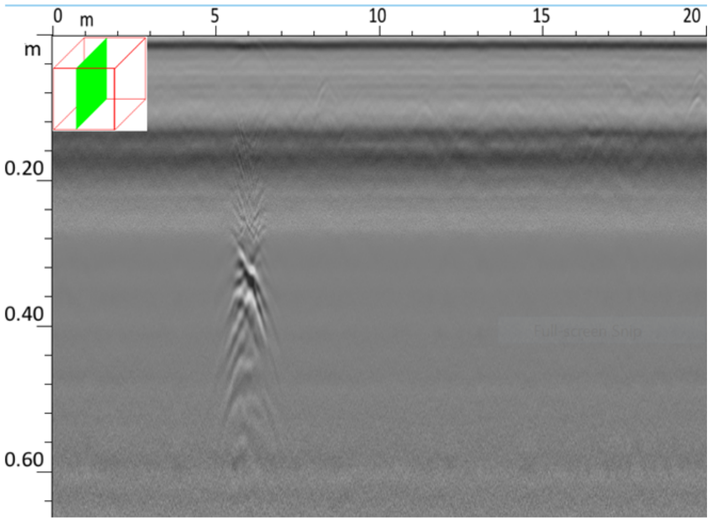

Figure 15. Y aspect radargram for the anomaly in Grid008.

Termite activity is associated with graves in some environments (Parkinson, et.al., 2014), however, this does not appear to be the case here.

6.10. Grid009

No radar anomalies consistent with the presence of graves were observed in the 3D reconstruction for this grid.

6.11. Grid010

An anomaly consistent with the presence of a possible grave (approximately 1 m wide, 2,5 m long and 1,85 m deep) was observed at X6-7Y13,5-15.

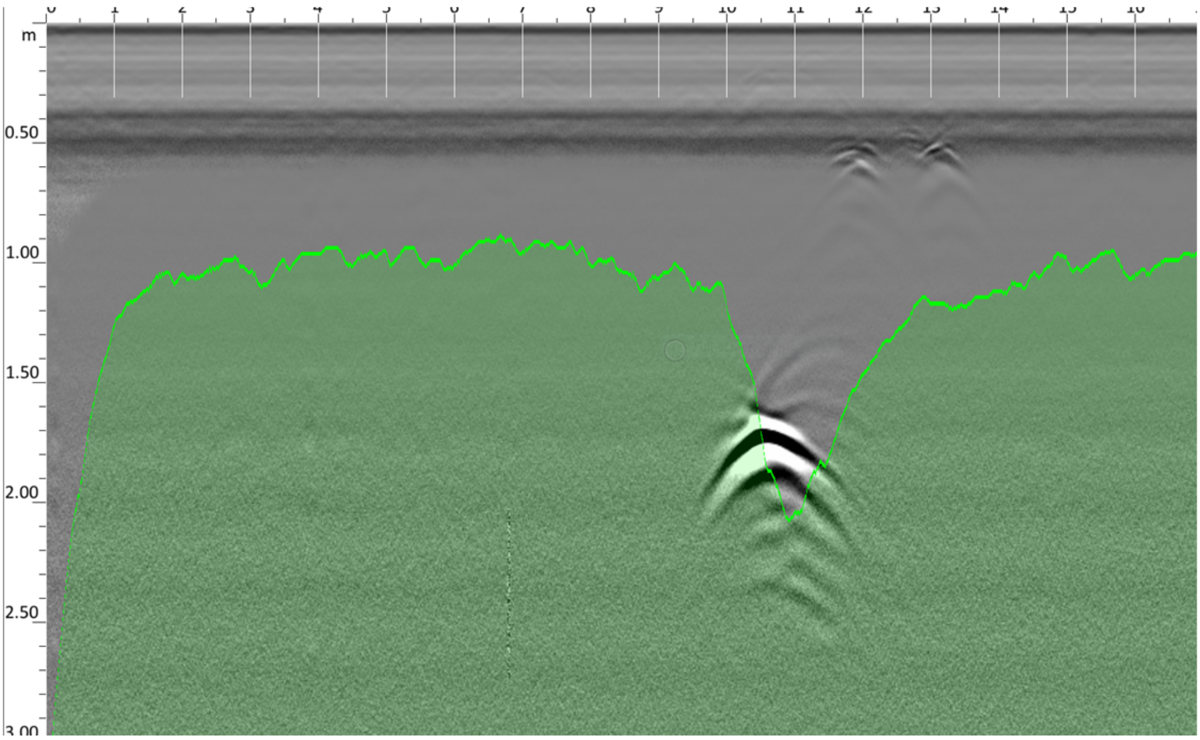

Figure 16. Anomaly consistent with a possible grave in Grid010.

6.12. Grid011

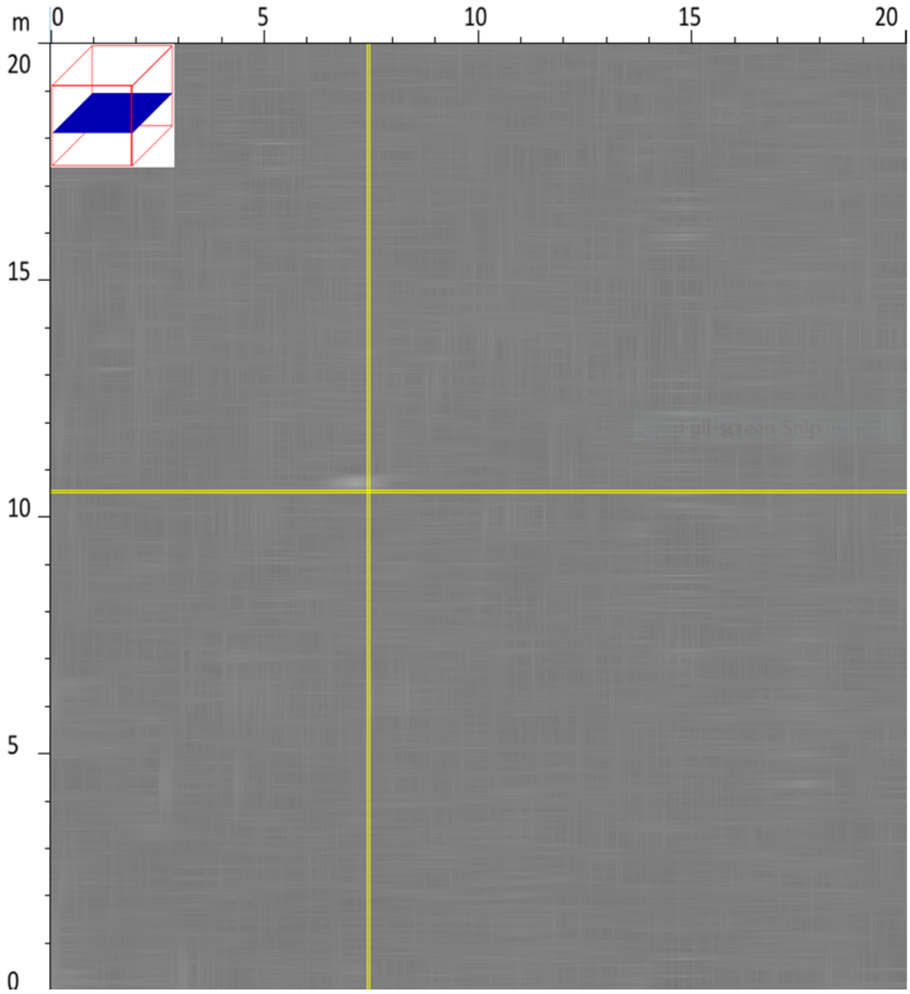

Figure 17. Grid011 3D visualization of data.

An anomaly presented in the 3D visualization of data for this grid.

X7,44Y9.47Z0,66 – This possible anomaly proved to be a data artefact when viewed in the Y aspect.

6.13. Grid012

No radar anomalies consistent with the presence of graves were observed in the 3D reconstruction for this grid.

6.14. Grid013

A possible anomaly observed in this grid at: X16,04Y2,00Z0,77 – Most probably a rock as observed in the Y aspect radargram.

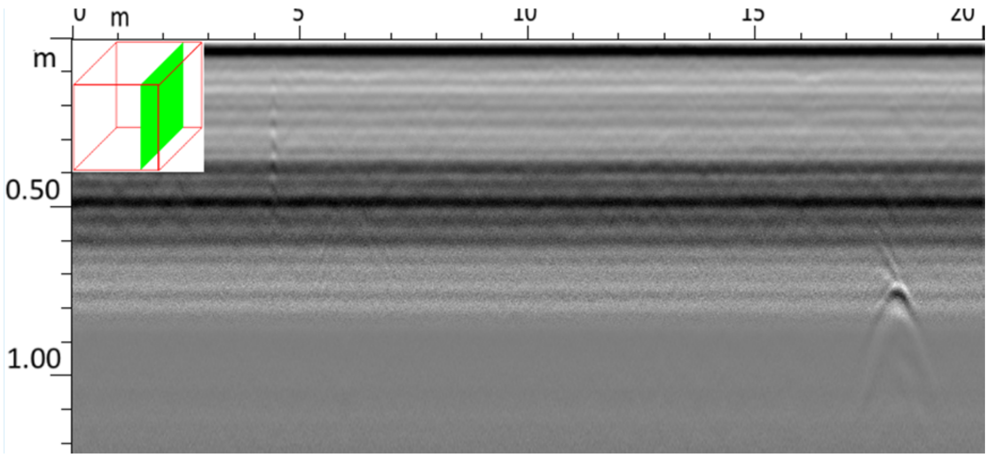

Figure 18. Grid013 Y profile radargram.

6.15. Grid014

No radar anomalies consistent with the presence of graves were observed in the 3D reconstruction for this grid.

6.16. Grid015

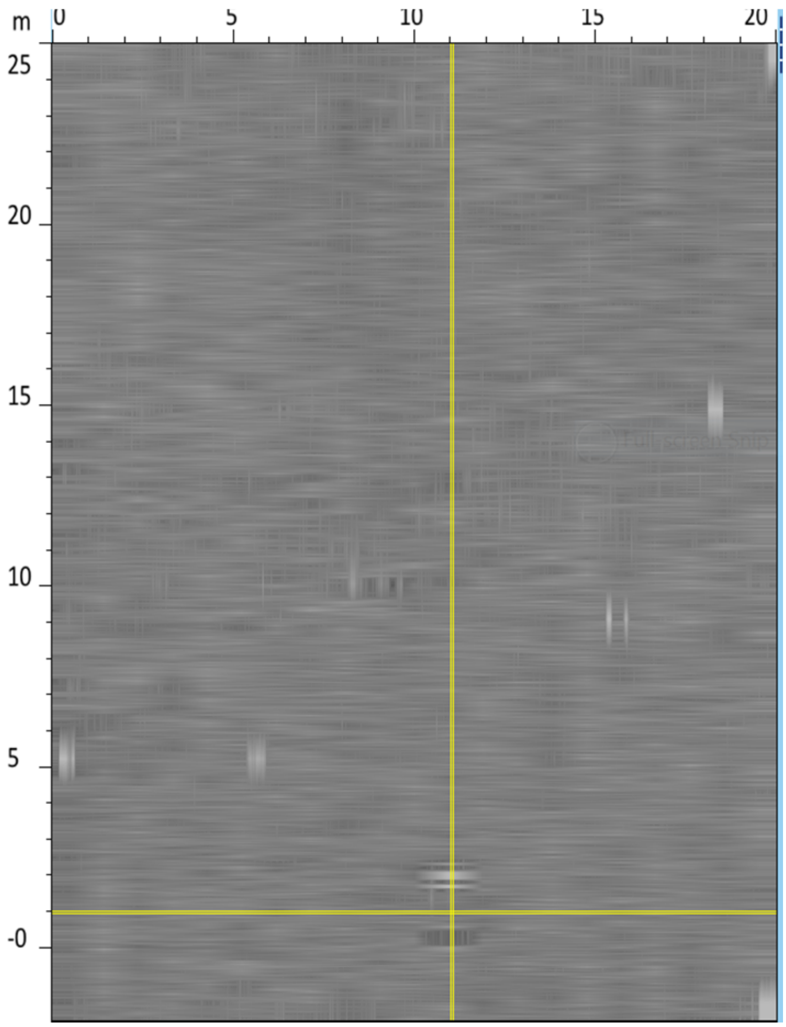

Figure 19. 3D visualization of data for Grid015.

An anomaly was observed at X11,04Y24,03Z0,78.

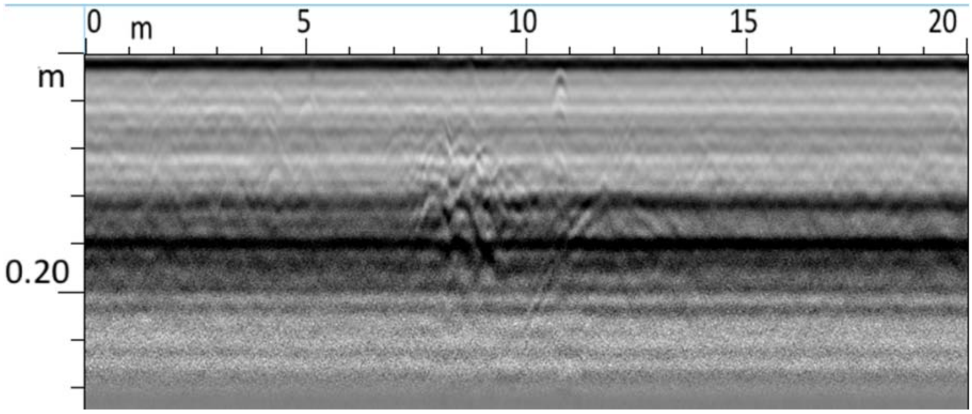

Figure 20. X profile for the anomaly in Grid015.

This anomaly is consistent with building remains and is related to the habitation debris observed on the surface at this location.

6.17. Grid016

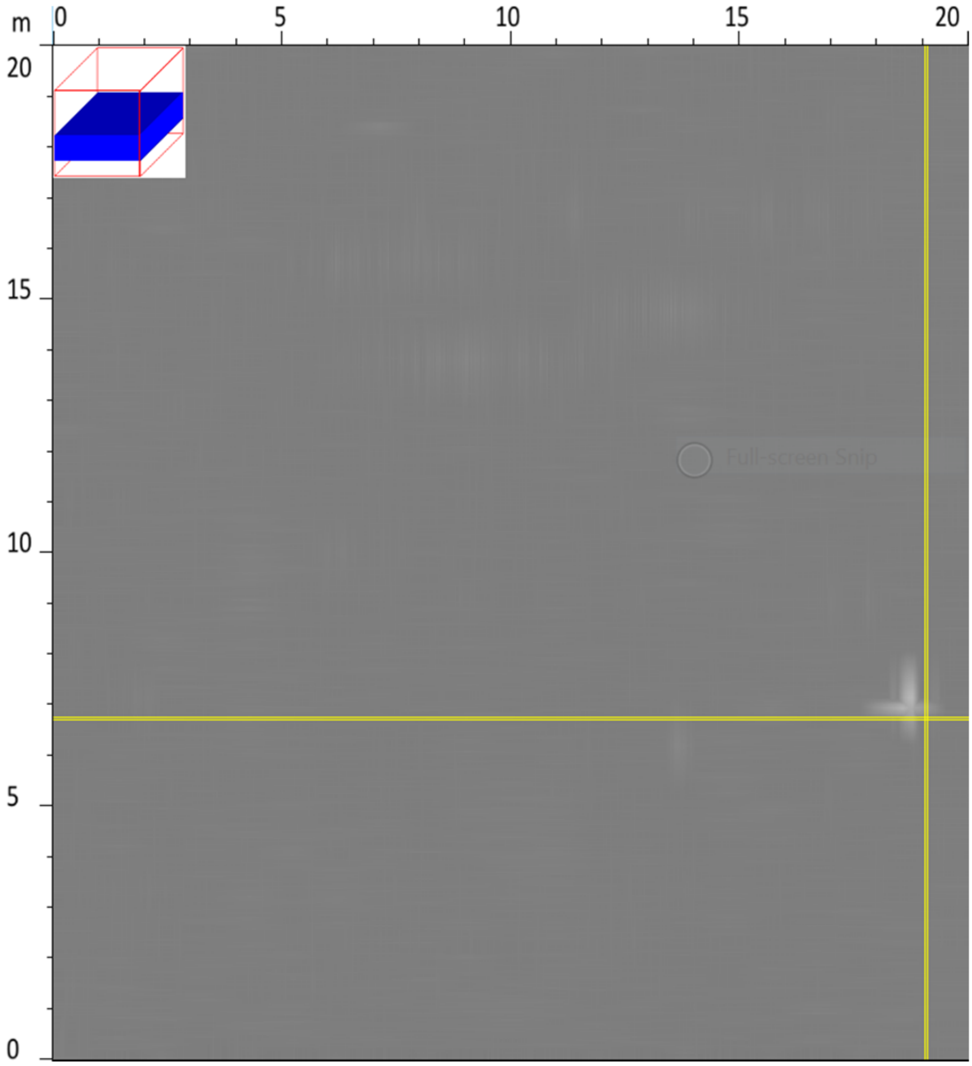

Figure 21. Grid016 3D visualization of data.

An anomaly was observed in the 3D visualization of data at X19,09Y13,29Z0,75.

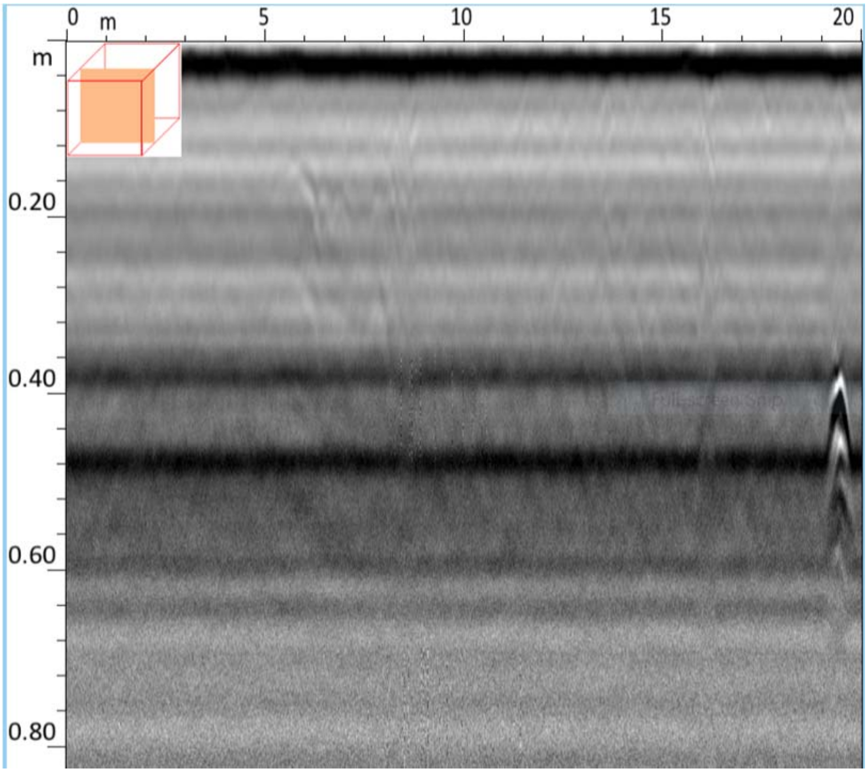

Figure 22. X aspect radargram for anomaly in Grid016.

This anomaly only occurs at a depth above approximately 0,6 m and are related to the habitation remains visible on the surface at this location. This is confirmed by the radar data profile for Grid016 X20.

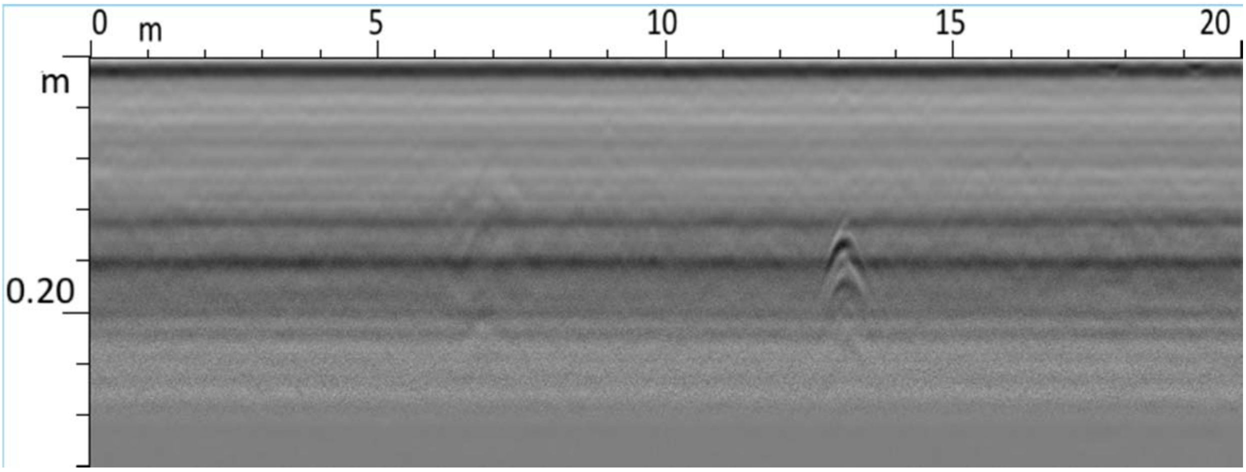

Figure 23. X profile at 20 m for Grid016.

6.18. Grid017

Anomalies were visible in the 3D visualization of data for this grid. However, when observing the profiles it is evident that these are data artefacts caused by antenna decoupling and poor odometer tracking as a result of the uneven surface in this part of the survey area and does not represent significant sub-surface anomalies.

6.19. Grid018

The uneven rock strewn surface in this part of the survey area is clearly visible in the upper (northern) part of the 3D visualization of data for this grid.

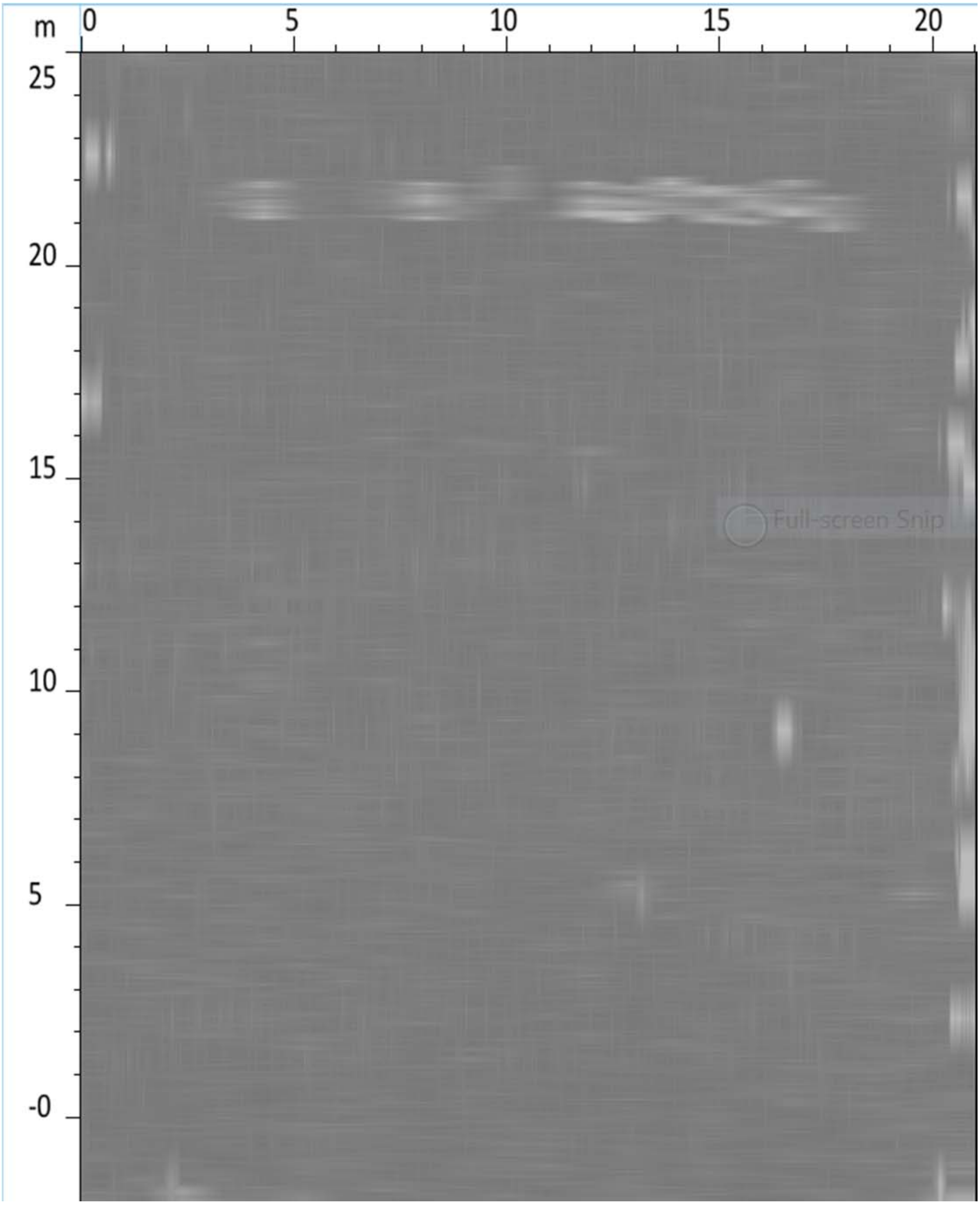

Figure 24. 3D visualization of data for Grid018.

An anomaly observed at X1,98Y1,00Z1,97 is also seen in the Y aspect but shows no continuation to the surface and can therefore not represent a possible grave.

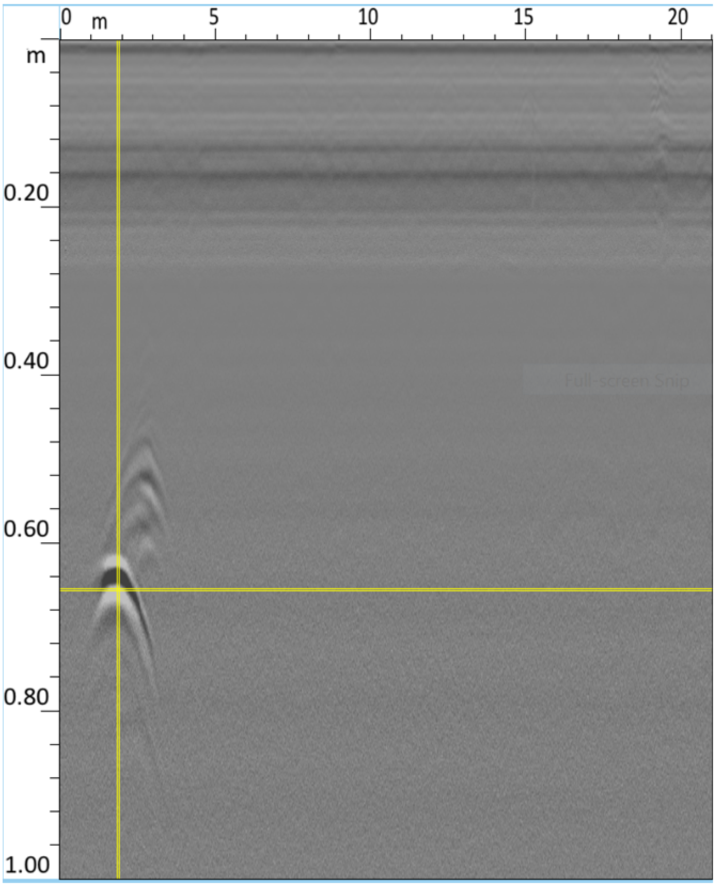

Figure 25. Y profile radargram for an anomaly in Grid0018.

6.20. Line012 X13,68Z1,222

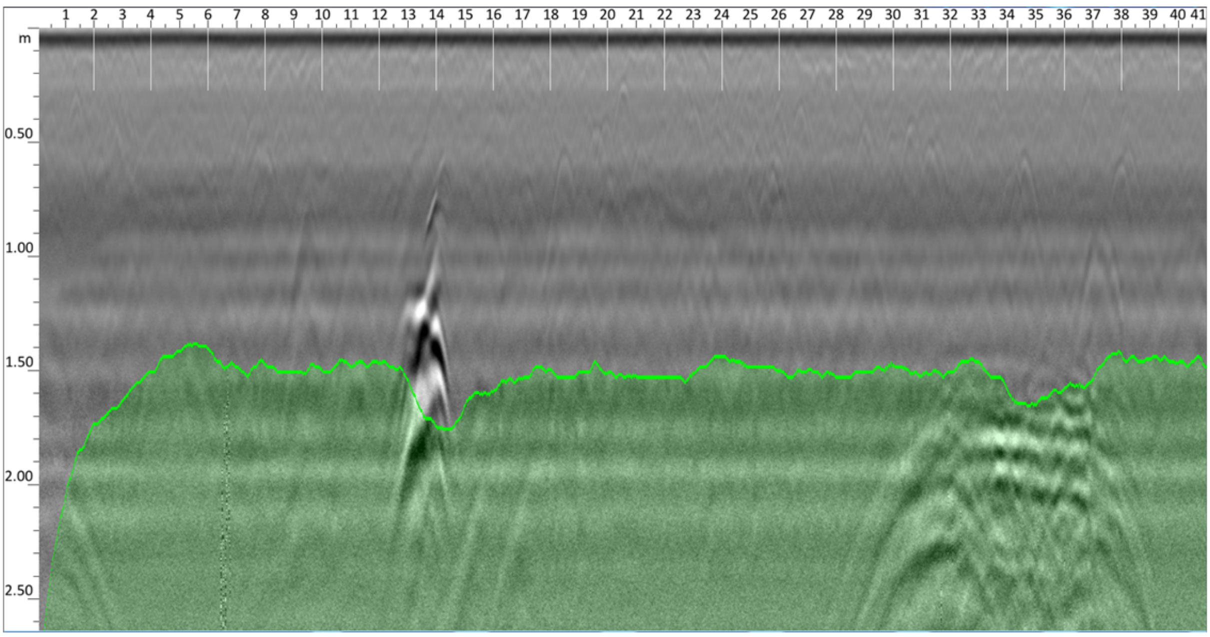

This anomaly only occurs in this profile and can therefore not be consistent with a possible grave due to its small size. The anomalies observed here were most likely the result of differences in water penetration and subsurface retention of water from the continuous spraying of water on the road for dust suppression.

6.21. Line015 X25,78Z1,118; X27,762Z1,450 and Line016 X17,38Z1,151

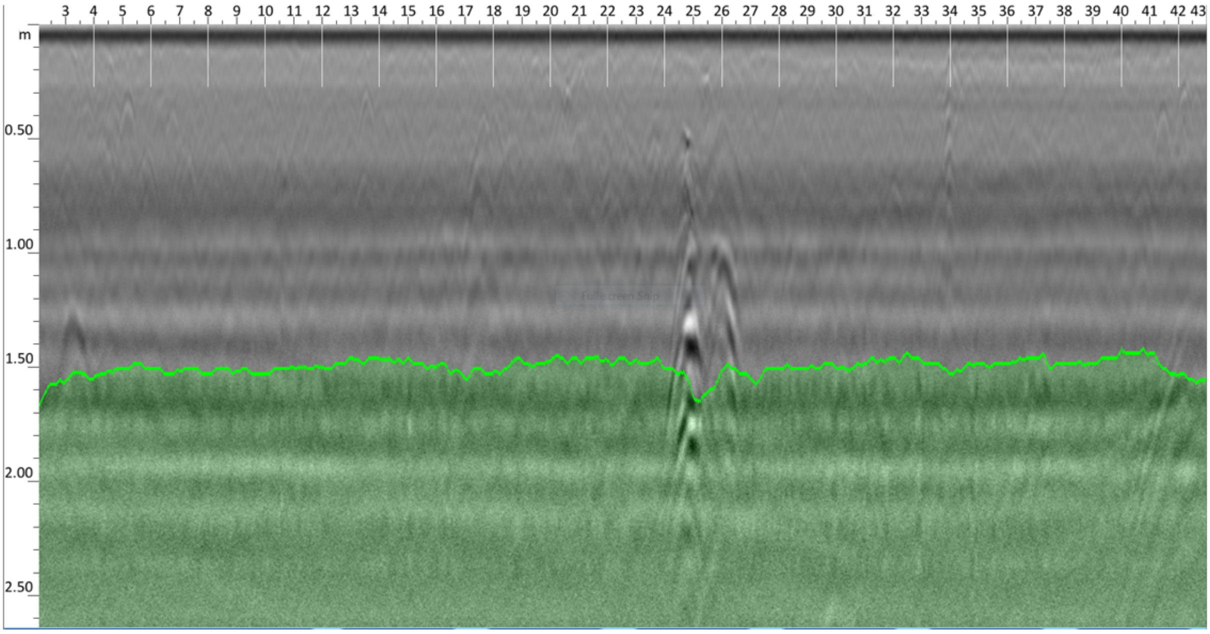

Figure 26. Anomaly observed in Line015.

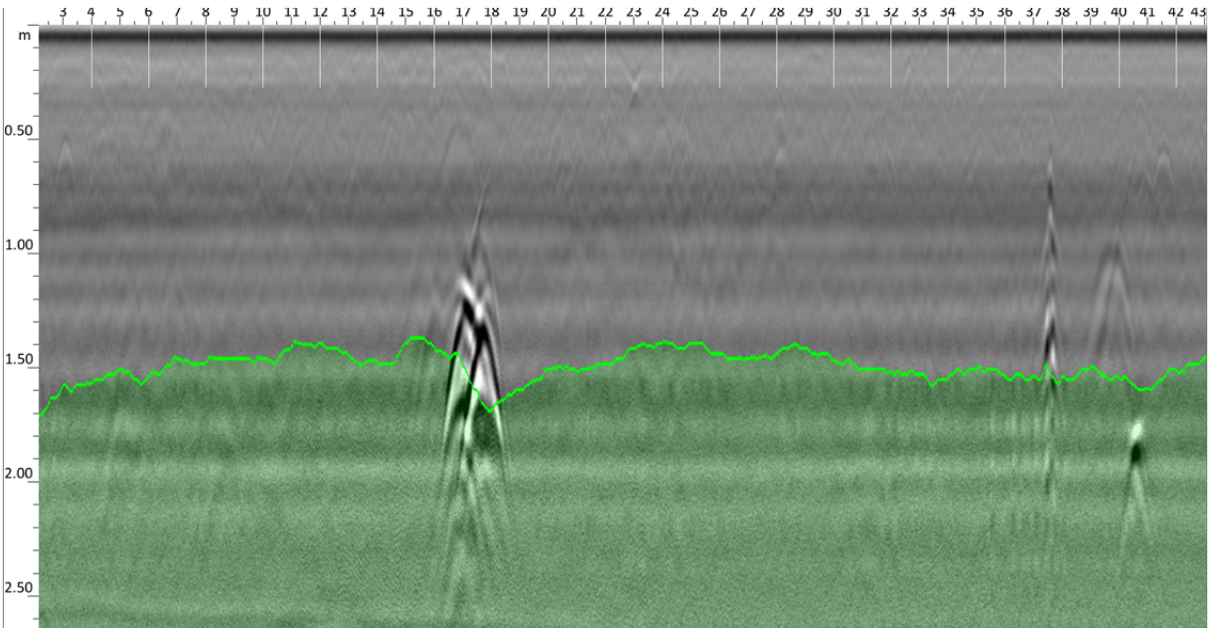

Figure 27. Anomaly observed in Line016.

This anomaly occurs over two profile lines and could therefore be the correct size for a possible grave, however the typical radar signature of an anomaly consistent with a possible grave is not visible. The anomalies observed here were most likely the result of differences in water penetration and subsurface retention of water from the continuous spraying of water on the road for dust suppression.

6.22. Line017 X26,4Z1,365

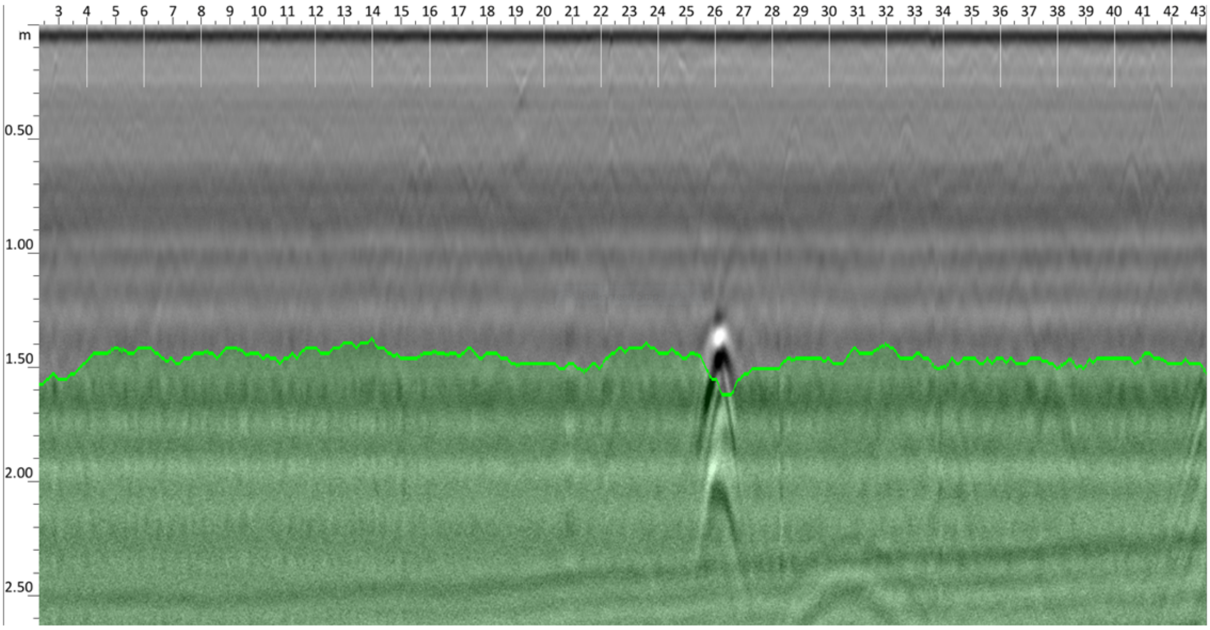

Figure 28. Anomalies visible in Line017.

This anomaly only occurs in this profile and can therefore not be consistent with a possible grave due to its small size. The anomalies observed here were most likely the result of differences in water penetration and subsurface retention of water from the continuous spraying of water on the road for dust suppression.

6.23. Line018 X14,62Z0,769-2,304 and Line019 X28,1Z1,049-2,134

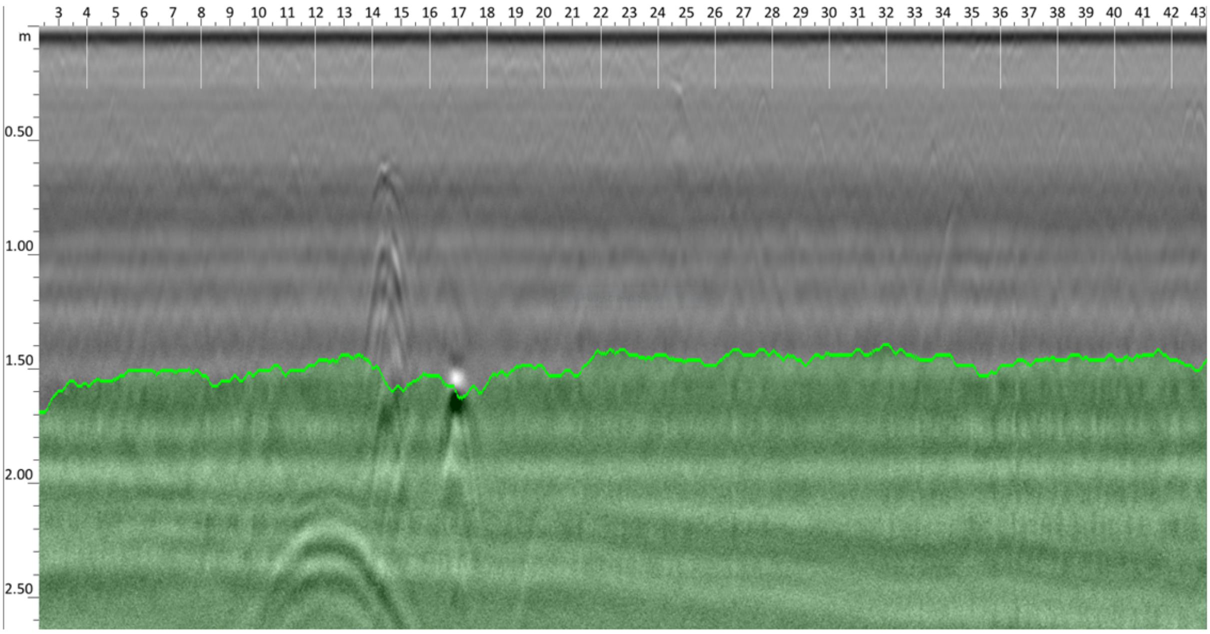

Figure 29. Anomalies in Line018.

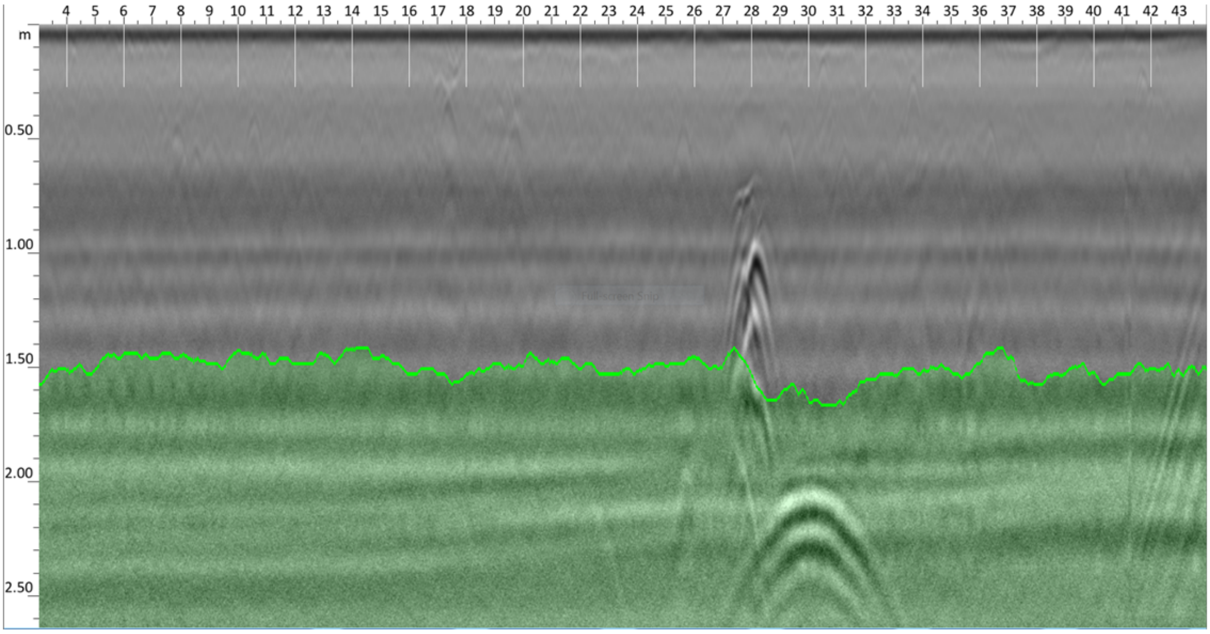

Figure 30. Anomalies visible in Line019.

This anomaly occurs over two profile lines and could therefore be the correct size for a possible grave, however the typical radar signature of an anomaly consistent with a possible grave is not visible. The anomalies observed here were most likely the result of differences in water penetration and subsurface retention of water from the continuous spraying of water on the road for dust suppression.

7. FINDINGS AND RECOMMENDATIONS

7.1. Anomalies consistent with the presence of possible graves

It is advised that the following localities be ground truthed through archaeological excavation to ascertain whether there are graves present:

1. An anomaly consistent with the possible presence of a grave was observed at Grid10 X6-7Y13,5-15 or grid position X6-8Y93,5-95 taken from point SOP3 as origin and oriented to SOP2(Y) and SOP4(X) (Refer Figure 2, Figure 3 and Figure 31). It should be considered whether this might be Grave 11A of the graves identified for the Platreef Project.

7.2. Localities that might contain human remains

A watching brief at the commencement of construction is advised for the following localities due to the fact that the graves of young children and babies might be present in the house ruins that occur here:

1. Surface indications of previous habitation and subsurface radar anomalies consistent with the presence of building ruins were observed at Grid015 X11,04Y24,03Z0,78 or rid position X31Y1044 from SOP3 (Figure 2, Figure 3 and Figure 31).
2. And Grid016 X19,09Y13,29Z0,75 or X56Y73 from SOP3 (Figure 2, Figure 3 and Figure 31Figure 31. Map indicating the localities that require action.).

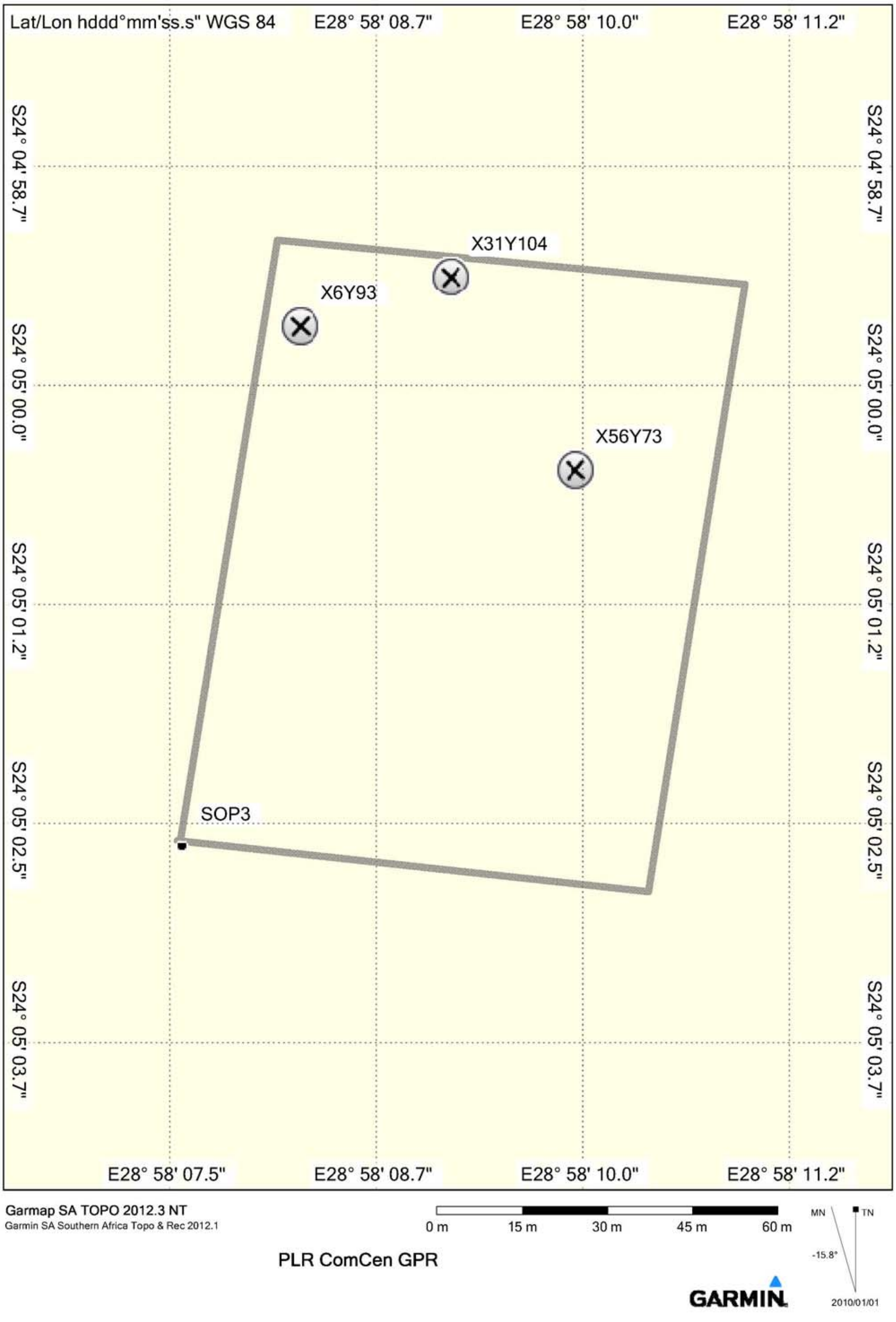

Figure 31. Map indicating the localities that require action.

BIBLIOGRAPHY

Dojack, L., 2012. Ground Penetrating Radar Theory, Data Collection, Processing, and Interpretation: A Guide for Archaeologists. (Doctoral dissertation, University of British Columbia).

Doolittle JA, Bellantoni NF. The search for graves with ground-penetrating radar in Connecticut. Journal of Archaeological Science. 2010; 37(5): 941-949.

Dupras, T.L., Schultz, J. J., Wheeler, S. H. and Williams, L. J. 2012. Forensic Recovery of Human Remains: Archaeological Approaches. 2 ed. Boca Raton: CRC Press.

Conyers, L.B. 2006. Ground-penetrating radar. In: J.K. Johnson (ed.), Remote Sensing in Archaeology: an Explicitly North American Perspective. Tuscaloosa, Alabama: The University of Alabama.

Fiedler, S., Illich, B., Berger, J. and Graw, M. 2009. The effectiveness of ground-penetrating radar surveys in the location of unmarked burial sites in modern cemeteries. Journal of Applied Geophysics, 68(3): 380-385.

Hansen, J.D., Pringle, J.K. and Goodwin, J. 2014. GPR and bulk ground resistivity surveys in graveyards: locating unmarked burials in contrasting soil types. Forensic Science International, 237: 14-29.

http://www.geophysical.com/utilityscandf.htm (Accessed 2015/11/02)

Molina, C. M., J. K. Pringle, M. Saumett, and O. Hernández, 2015. Preliminary results of sequential monitoring of simulated clandestine graves in Colombia, South America, using ground penetrating radar and botany. Forensic Science International, 248: 61-70.

Novo, A., Lorenzo, H., Rial, F.I. and Solla, M. 2011. 3D GPR in forensics: Finding a clandestine grave in a mountainous environment. Forensic Science International, 204: 134-138.

A.H. Parkinson, S. Van der Walt, P.S. Randolph-Quinney, P. Dirks, B. Billings, M. Steyn, W.C. Nienaber and A. Esterhuisen. Application of forensic taphonomy and entomology to the analysis of South African burial systems. Poster presentation: 14th Congress of the Pan African Archaeological Association for Prehistory and Related Studies, 22nd Biennial Meeting of the Society of Africanist Archaeologists 2014.

Pringle, J. K., J. Jervis, J. P. Cassella, and N. J. Cassidy. 2008. Time-Lapse Geophysical Investigations over a Simulated Urban Clandestine Grave. Journal of Forensic Science, 53: 1405-1416.

Schultz, J. J. 2008. Sequential Monitoring of Burials Containing Small Pig Cadavers Using Ground Penetrating Radar. Journal of Forensic Science. 53: 279-287.

Schultz, J.J. 2012. The Application of Ground-Penetrating Radar for Forensic Grave Detection. In: D. Dirkmaat (ed.), A companion to forensic anthropology. John Wiley & Sons.

Schultz, J. J., and M. M. Martin. 2012. Monitoring controlled graves representing common burial scenarios with ground penetrating radar. Journal of Applied Geophysics, 83: 74-89.